



Structure-based design, semi-synthesis and anti-inflammatory activity of tocotrienolic amides as 5-lipoxygenase inhibitors

Chau-Phi Dinh, Alexia Ville, Konstantin Neukirch, Guillaume Viault, Veronika Temml, Andreas Koeberle, Oliver Werz, Daniela Schuster, Hermann Stuppner, Pascal Richomme, et al.

► To cite this version:

Chau-Phi Dinh, Alexia Ville, Konstantin Neukirch, Guillaume Viault, Veronika Temml, et al.. Structure-based design, semi-synthesis and anti-inflammatory activity of tocotrienolic amides as 5-lipoxygenase inhibitors. European Journal of Medicinal Chemistry, 2020, 202, pp.112518. 10.1016/j.ejmech.2020.112518 . hal-02884134

HAL Id: hal-02884134

<https://univ-angers.hal.science/hal-02884134>

Submitted on 18 Jul 2022

HAL is a multi-disciplinary open access archive for the deposit and dissemination of scientific research documents, whether they are published or not. The documents may come from teaching and research institutions in France or abroad, or from public or private research centers.

L'archive ouverte pluridisciplinaire **HAL**, est destinée au dépôt et à la diffusion de documents scientifiques de niveau recherche, publiés ou non, émanant des établissements d'enseignement et de recherche français ou étrangers, des laboratoires publics ou privés.



Distributed under a Creative Commons Attribution - NonCommercial 4.0 International License

Structure-based design, semi-synthesis and anti-inflammatory activity of tocotrienolic amides as 5-lipoxygenase inhibitors

Chau Phi Dinh^a, Alexia Ville^a, Konstantin Neukirch^{b,e}, Guillaume Viault^a, Veronika Temml^c, Andreas Koeberle^{b,e}, Oliver Werz^b, Daniela Schuster^d, Hermann Stuppner^c, Pascal Richomme^a, Jean-Jacques Helesbeux^{a*} and Denis Séraphin^a

^a SONAS, EA921, UNIV Angers, SFR QUASAV, Faculty of Health Sciences, Department of Pharmacy, 16 bd Daviers, 49045 Angers Cedex 01, France.

^b Department of Pharmaceutical/Medicinal Chemistry, Institute of Pharmacy, Friedrich-Schiller-University Jena, Philosophenweg 14, 07743 Jena, Germany.

^c Institute of Pharmacy/Pharmacognosy University of Innsbruck, 80/82 Innrain, 6020 Innsbruck, Austria.

^d Department of Pharmaceutical and Medicinal Chemistry, Paracelsus Medical University Salzburg, Strubergasse 21, 5020 Salzburg, Austria.

^e Michael Popp Research Institute, University of Innsbruck, Mitterweg 24, 6020, Innsbruck, Austria.

Keywords: Inflammation; 5-lipoxygenase; vitamin E; molecular docking; semi-synthesis; leukotrienes.

*Corresponding author:

Email: jean-jacques.helesbeux@univ-angers.fr

Abstract: Inflammation contributes to the development of various pathologies, e.g. asthma, cardiovascular diseases, some types of cancer, and metabolic disorders. Leukotrienes (LT), biosynthesized from arachidonic acid by 5-lipoxygenase (5-LO), constitute a potent family of pro-inflammatory lipid mediators. δ -Garcinoic acid (δ -GA) (**1**), a natural vitamin E analogue, was chosen for further structural optimization as it selectively inhibited 5-LO activity in cell-free and cell-based assays without impairing the production of specialized pro-resolving mediators by 15-LO. A model of semi-quantitative prediction of 5-LO inhibitory potential developed during the current study allowed the design of 24 garcinamides that were semi-synthesized. In accordance with the prediction model, biological evaluations showed that eight compounds potently inhibited human recombinant 5-LO ($IC_{50} < 100$ nM). Interestingly, four compounds were substantially more potent than **1** in activated primary human neutrophils assays. Structure - activity relationships shed light on a supplementary hydrophobic pocket in the allosteric binding site that could be fitted with an aromatic ring.

I. Introduction

Inflammation is an adaptive response of the immune system triggered by exogenous harmful stimuli or damaged tissues to maintain homeostasis of the body [1]. This process is involved in the development of various pathologies, e.g. asthma, cardiovascular diseases, some types of cancer, and metabolic disorders [2–5]. Inflammatory lipid mediators play a key role in the cascade response including the accumulation of leukocytes and the leakage of plasma from small vessels to inflamed tissues. 5-Lipoxygenase (5-LO)-derived leukotrienes (LTs) represent a class of pro-inflammatory lipid mediators derived from arachidonic acid (AA) [6]. 5-LO, a non heme iron-containing dioxygenase, is the key enzyme in LT biosynthesis which catalyses the oxidation of AA at C-5 position, yielding the intermediate (*S*)-5-hydroperoxyeicosatetraenoic acid (5-HPETE), and its dehydration to leukotriene A₄ (LTA₄) [7]. This derivative is rapidly transformed by LTA₄ hydrolase to LTB₄ or by microsomal glutathione-S-transferase to LTC₄ and then further metabolized to the cysteinyl-LTs LTD₄ and LTE₄.

Due to the importance of LTs in the pathogenesis of inflammation-related diseases, 5-LO has been identified as a key target for the development of new therapeutics [8]. Despite intensive research over the past 30 years in order to find selective and potent 5-LO inhibitors, zileuton, which was approved by the FDA in 1996, is the only drug targeting this enzyme [9,10]. Besides, numerous synthetic agents as well as naturally occurring compounds have been identified as 5-LO inhibitors, but most of them were neither sufficiently active nor selective against 5-LO, lacked *in vivo* efficiency, and/or were afflicted with severe side effects [11].

In the frame of the Drugs from Nature Targeting Inflammation (DNTI) program, anti-inflammatory vitamin E derivatives were identified [12–14]. Originally discovered in 1922 by Evans and Bishop, vitamin E is an essential fat-soluble vitamin encompassing 8 naturally occurring compounds classified in 2 subfamilies, namely tocopherols and tocotrienols [15,16].

Endogenous metabolites of vitamin E selectively inhibited the biosynthesis of 5-LO-derived lipid mediators without impairing the production of 15-LO-derived leukotrienes, key mediators involved in the resolution phase of inflammation. Among them, natural δ -garcinoic acid (δ -GA, **1**) (scheme 1), an ω -oxidized tocotrienol, inhibited human recombinant 5-LO and LTs biosynthesis by human primary polymorphonuclear leukocytes (PMNL) ($IC_{50} = 57 \pm 9$ nM and 345 ± 73 nM, respectively) [17]. Recently, this acid was also identified as a selective agonist of pregnane X receptor [18].

Due to its potency at low nanomolar concentrations, δ -GA (**1**) was selected as a hit to develop further 5-LO inhibitors as well as to investigate the structure-activity relationships (SAR) of this class of compounds. First, the phenolic function of **1** was modified to give ester or ether derivatives, but a complete loss of inhibitory activity was observed (data not shown). Therefore, this phenolic function is essential for 5-LO inhibition. Next, modulation of the acidic ω -function of **1** was investigated. On one hand, reduction of carboxylic acid to the corresponding primary alcohol led to a less active compound ($IC_{50} = 147 \pm 54$ nM). On the other hand, pull-down experiment with immobilized-GA using Toyopearl AF Amino 650 allowed the fishing of 5-LO. Moreover, tocotrienols classically underwent side-chain degradation starting with ω -oxidation followed by a series of β -oxidation leading to short-chain metabolites excreted into urine [19]. Thus, chemical modification of terminal carboxylic acid might limit this process and enhance tocotrienol half-life. This prompted us to design a series of new garcinamides and to evaluate their 5-LO inhibitory activity.

In this paper, a molecular docking study, relying on the preliminary identification of a new allosteric binding site, was performed using an in-house database of vitamin E derivatives to build a semi-quantitative IC_{50} prediction workflow [17]. Then, a concise semi-synthesis of new garcinamides is described. Moreover, their inhibitory activity against 5-LO in cell-free and cell-based assays is evaluated, and SAR are discussed.

II. Results and discussion

1. Molecular docking

The combination of molecular docking simulations and site-directed mutagenesis studies reported previously showed the importance of Trp102 within the novel allosteric binding site of 5-LO [17]. Trp102 is located between the regulatory C2-like and the catalytic domains (Figure 1). Its indole ring is bulked in the cavity formed by these two domains and surrounded by other amino acids such as Gln15 and Asp170. The cavity is stretched toward Val110. Finally, it is defined by 11 residues from both domains of 5-LO. δ -GA **1** has been docked into this cavity using default parameters of GOLD [20]. Its best-ranked pose showed two intermolecular hydrogen bonds: one involved the ligand's phenolic oxygen and the NH of the indole of Trp102; the other linked the amide function of Val110's backbone and the ligand's carbonyl group. Additionally, the phytyl-like side chain and both methyl substituents of the chromanol formed hydrophobic interactions with Val110, His130, Lys133, Tyr383, and Arg401.

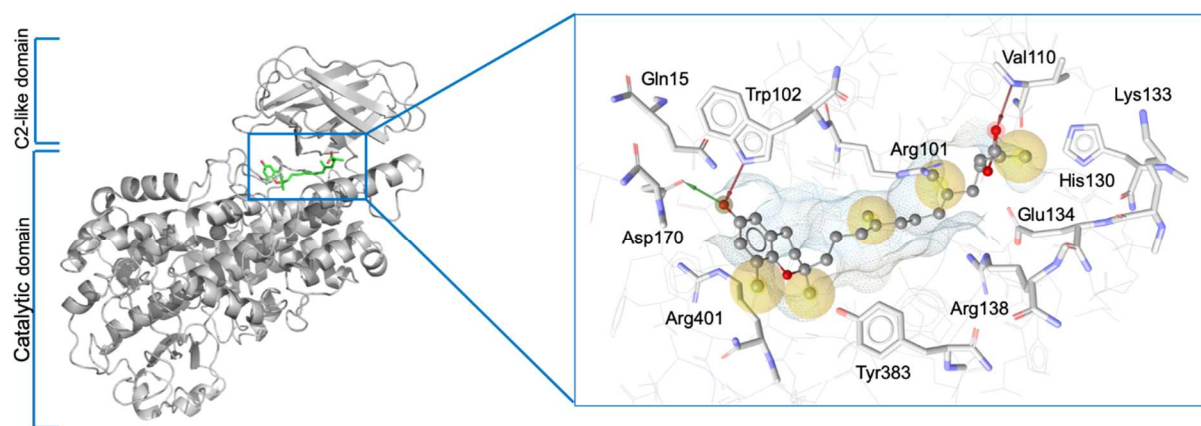


Figure 1 : Molecular docking pose of δ -GA **1** in the allosteric binding site of 5-LO. Hydrogen bonds are shown as red and green arrows, hydrophobic contacts as yellow spheres.

Among the in-house tocotrienol library already evaluated against 5-LO (cell-free) assay, 17 derivatives, including δ -GA **1**, exhibiting IC_{50} values ranging from 50 nM to 1722 nM were selected to build the training set (Supplementary data). These compounds were then docked into the allosteric binding site using the workflow previously used (see above) to optimize the *in silico* model of 5-LO. The output fitness scores calculated by the built-in CHEMPLP scoring function in GOLD – an empirical scoring function that takes into account the contribution of hydrogen bonds, non-polar interactions and metal chelation energy calculated from the distance of involved heavy atoms – did not significantly vary among the investigated compounds [21]. Moreover, no linear correlation between these scores and the measured pIC_{50} values of these compounds could be established. Judging from the scoring function, a strong affinity for the allosteric binding site was predicted for all compounds. This *in silico* result was not in accordance with biological data that in general cannot often be directly translated to binding affinity, since other effects, like solubility or off-target interactions may prevent the molecule from reaching the intended binding site. However, aiming for a semi-quantitative structure-activity relationship, the workflow was refined, and the scoring function was modified to reflect the experimentally established importance of key hydrogen bonds.

In a detailed analysis of the docking results, we found that poses with H-bonds were calculated only for six compounds out of the 17 derivatives from the training set. The calculation run by this first model mainly took into account the hydrophobic interactions with residues Val110, Lys133 and Tyr383, leaving only a very limited contribution of hydrogen bonds to the fitness score. Besides, the lack of repulsion force observed in the best-ranked poses of all 17 compounds led to unexpectedly high fitness scores regarding to biological data. Thus, docking parameters were modified to increase the contribution of hydrogen bonds in the calculation. An advanced setting, “Protein HBond”, from GOLD docking

algorithm is dedicated to search solutions that featured intermolecular hydrogen bonds involving pre-defined protein atoms. The exhaustive analysis of docking poses of the training set allowed the identification of five structural moieties which formed hydrogen bonds with the ligands: the indole of Trp102, the carboxyl group of Glu134, the NH of Val110, the carboxyl group of Asp170 and the guanidine moiety of Arg401. Hence, the weight of each hydrogen bond contribution was tuned in order to emphasize the importance of each interaction leading to a correlation with $R^2 = 0.86$ (Figure 2) between the calculated and the measured pIC_{50} values (See experimental section IV.1). A first verification of this workflow with a test set of 20 vitamin E derivatives previously evaluated in cell-free 5-LO activity assay also yielded satisfactory correlation ($R^2 = 0.65$) (Supplementary Data). A second approach was developed with the distribution of the compounds from the test set into four groups depending on their pIC_{50} value: highly active ($IC_{50} \leq 100$ nM), active (100 nM $< IC_{50} \leq 300$ nM), moderately active (300 nM $< IC_{50} \leq 1000$ nM), and inactive ($IC_{50} > 1000$ nM). Then, the compounds were also categorized into these groups based on the calculated pIC_{50} values, obtained from the compounds' fitness scores. A one-way ANOVA test showed that no significant difference between both distributions was observed (Supplementary Data). These two verifications validated the *in silico* workflow. It was thus applied to the design of 5-LO inhibitors based on the garcinoic acid scaffold.

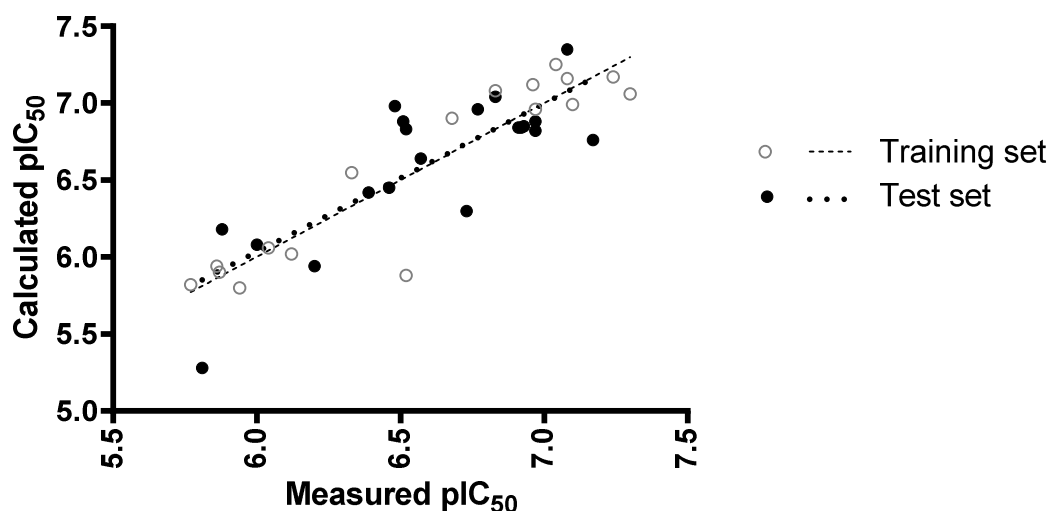


Figure 2 : Linear regression between measured and calculated pIC_{50} values of both training and test sets.

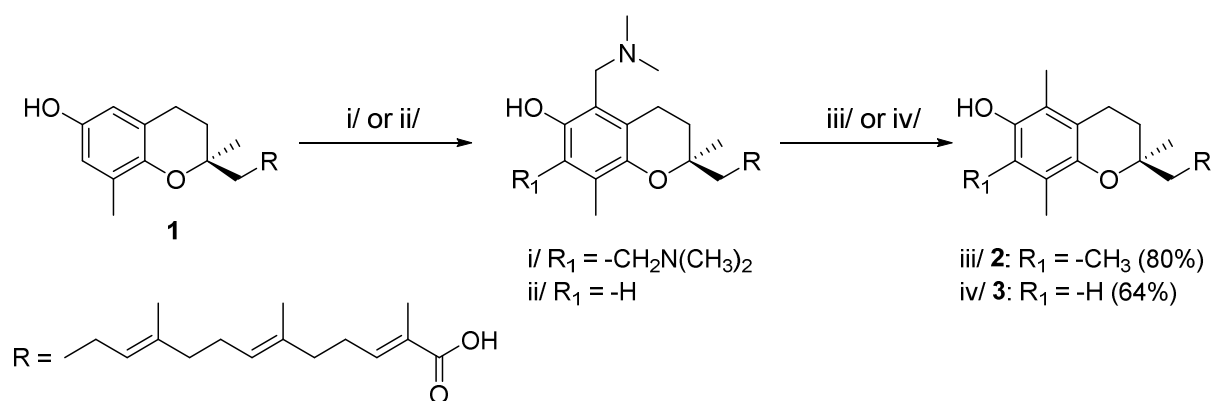
Despite their high anti-inflammatory activity through the inhibition of 5-LO, ω -oxidized vitamin E analogues, including δ -GA **1**, undergo the classical oxidative metabolism of this class of derivatives [22]. As a result, their bioavailability is questionable. Recently, the semi-synthesis and the anti-inflammatory activity of the benzylamide of δ -GA were reported [17]. This result

prompted us to explore the pharmacological potential of other garcinamides. It can be assumed that these analogues could be less prone to the oxidative metabolism of the phytyl-like side chain. Moreover, designing garcinamides opened the possibility to explore a chemical space with potentially new interactions with other amino acid residues from the 5-LO allosteric binding site. Therefore, the aforementioned docking procedure was used to predict the 5-LO inhibitory activity of *in silico* designed garcinamides. In accordance with the concentration ranges used in the cell-free 5-LO assay, the compounds from this virtual library were distributed to four groups of predicted activity: highly active ($IC_{50} \leq 100$ nM), active (100 nM $< IC_{50} \leq 300$ nM), moderately active (300 nM $< IC_{50} \leq 1000$ nM), and inactive ($IC_{50} > 1000$ nM).

Among this virtual library of 117 garcinamides (Supplementary data), the docking results highlighted 24 promising compounds predicted as moderately to highly active. They were semi-synthesized and subjected to biological assays to validate the molecular model and to understand further the SARs (Table 1).

2. Semi-synthesis

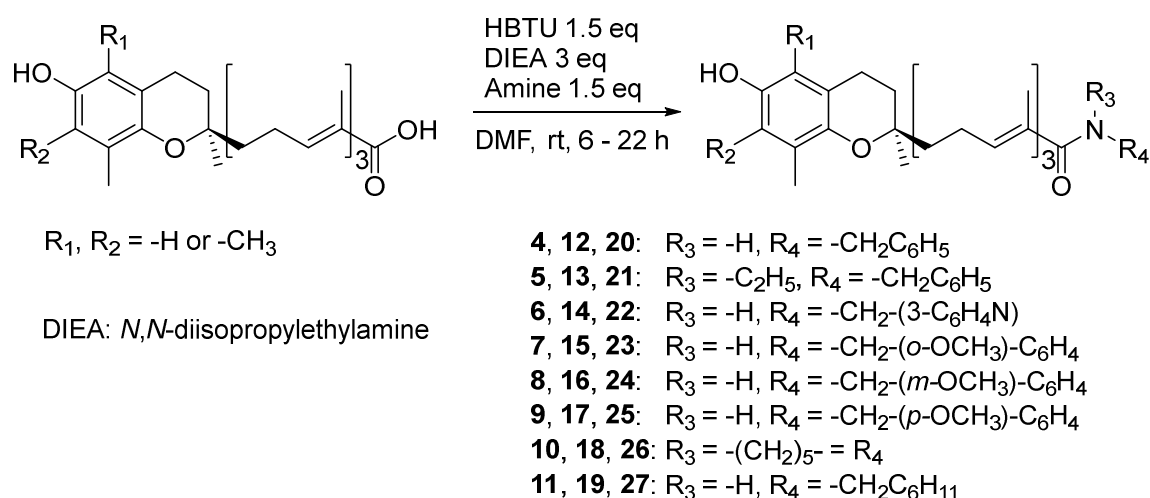
δ -GA **1** was extracted from *Garcinia kola* nuts according to a previously described procedure [23]. α - and β -GA isoforms **2** and **3** were prepared in accordance with a previously established two-step method, with some optimizations giving 80 and 64% overall yield respectively [14]. It is worth mentioning that access to the β -isoform is a one-pot procedure and the reduction of intermediate is achieved at reflux in ethanol (Scheme 1).



Scheme 1: Semi-synthesis of α - and β -garcinoic acids.
i/ $(\text{CH}_2\text{O})_n$ (20 eq), TMDA (20 eq), dioxane 140 °C, MW, 40 min; *ii/* $(\text{CH}_2\text{O})_n$ (3 eq), TMDA (3 eq), EtOH 120 °C, MW, 20 min; *iii/* NaBH_3CN (30 eq), EtOH, reflux, 16 h; *iv/* NaBH_3CN (8 eq), EtOH, reflux, 14 h.

Amide synthesis involved the activation of the carboxylic function by an electron-withdrawing group and the attack of an amino group onto the activated form to give the expected function [24,25]. Various coupling agents were evaluated for the reaction of δ -GA (**1**) with 4-methoxybenzylamine. Among them, *O*-(benzotriazol-1-yl)-1,1,3,3-tetramethyluronium

hexafluorophosphate (HBTU) was chosen [26]. The three isoforms of GA were coupled with 8 commercially available amines to afford, sometimes after tedious purification, 24 garcinamides **4** – **27** (29 – 88% yield) (Scheme 2).



Scheme 2: Synthesis of the garcinamide library.

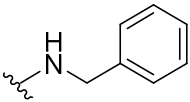
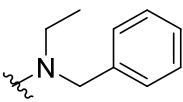
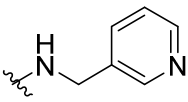
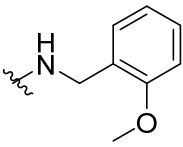
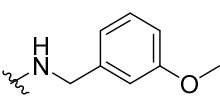
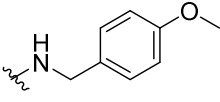
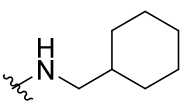
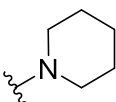
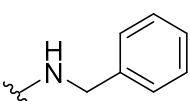
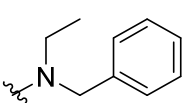
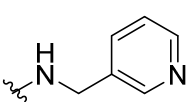
3. Evaluation of 5-LO inhibitory activities in cell-free and cell-based assays

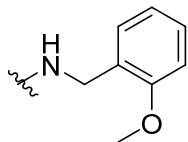
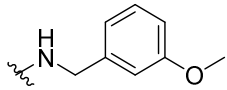
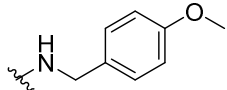
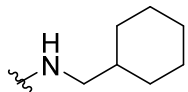
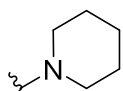
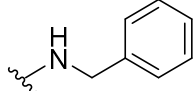
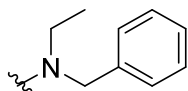
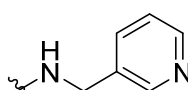
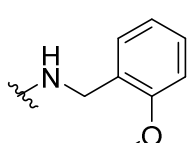
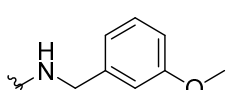
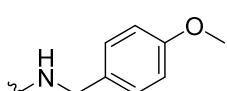
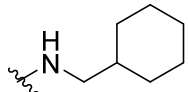
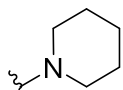
The effect of garcinamides on 5-LO was studied in a cell-free assay using the human recombinant enzyme and in a cell-based assay with activated human PMNL, which convert the supplemented substrate arachidonic acid into the 5-LO products LTB₄, its isomers and 5-H(P)ETE. We expect substantial differences between the potency of garcinamides in cell-free and cell-based assays because SARs for 5-LO inhibition likely overlay with those for cellular uptake or retention, as recently shown for long-chain vitamin E metabolites [17].

Calculated and measured IC₅₀ values of GA isoforms (**1**, **2**, **3**) and garcinamides **4** – **27** are reported in Table 1, with zileuton as the reference [9].

Table 1: Calculated and measured IC₅₀ values. Data are expressed as means ± SEM, n = 3 – 4.

Cpd	Structures			Predicted group*	IC ₅₀ 5-LO	Matched prediction	IC ₅₀ PMNL
	R ₁	R ₂	R ₃		[nM] (remaining activity (%) at 1 μM)		[nM] (remaining activity (%) at 3 μM)
1	H	H	OH	I	57 ± 9	✓	345 ± 73

2	CH ₃	CH ₃	OH	II	401 ± 78		1702 ± 520
3	CH ₃	H	OH	II	154 ± 38	✓	312 ± 110
4	H	H		I	50 ± 23	✓	303 ± 122
5	H	H		III	65 ± 19		525 ± 70
6	H	H		I	77 ± 6	✓	415 ± 109
7	H	H		I	76 ± 2	✓	>3000 (62 ± 4)
8	H	H		I	115 ± 15		>3000 (60 ± 1)
9	H	H		I	94 ± 9	✓	187 ± 58
10	H	H		I	131 ± 17		561 ± 164
11	H	H		II	129 ± 25	✓	>3000 (74 ± 2)
12	CH ₃	CH ₃		II	595 ± 208		173 ± 64
13	CH ₃	CH ₃		II	623 ± 320		> 3000 (n.d.#)
14	CH ₃	CH ₃		II	210 ± 21	✓	563 ± 186

15	CH ₃	CH ₃		III	422 ± 77	✓	1379 ± 449
16	CH ₃	CH ₃		III	725 ± 254	✓	839 ± 290
17	CH ₃	CH ₃		II	572 ± 202		250 ± 8
18	CH ₃	CH ₃		II	210 ± 20	✓	315 ± 17
19	CH ₃	CH ₃		III	998 ± 157	✓	>3000 (51 ± 3)
20	CH ₃	H		II	538 ± 107		175 ± 66
21	CH ₃	H		II	171 ± 56	✓	432 ± 286
22	CH ₃	H		II	362 ± 58		401 ± 144
23	CH ₃	H		I	119 ± 40		>3000 (56 ± 4)
24	CH ₃	H		II	80 ± 3		997 ± 291
25	CH ₃	H		II	97 ± 9		724 ± 171
26	CH ₃	H		I	265 ± 13		1291 ± 152
27	CH ₃	H		II	>1000 (50 ± 6)		>3000 (72 ± 1)

*Highly active compounds (I), active compounds (II), and moderately active compounds (III) according to the predicted IC₅₀. # n.d.: not determined

As mentioned before during the development of the virtual model, vitamin E analogues were distributed into four groups: I (IC₅₀ ≤ 100 nM), II (100 nM < IC₅₀ ≤ 300 nM), III (300 nM < IC₅₀ ≤ 1000 nM), and IV (IC₅₀ > 1000 nM). The *in silico* workflow was first applied to GA isoforms (**1**, **2**, **3** – Table 1). The predicted values for **1** and **3** (group I and II respectively) were in accordance with experimental data (cell-free 5-LO assay) while α-GA **2**, classified into group II after docking procedure, was found moderately active (group III). δ-Garcinamides (**4** – **11**) were mainly assigned to group I. The corresponding α-isoforms **12** – **19** belong to group II and III. Eventually, β-garcinamides (**20** – **27**) were part of group II.

Amides **4** – **27** were evaluated for 5-LO inhibition (cell-free assay) and their measured IC₅₀ values ranged from 50 ± 23 up to 1000 nM. Among these 24 compounds, the IC₅₀ values were correctly predicted for 11 compounds homogeneously distributed over the groups I to III. This first predictive model built to categorize novel GA analogues into different 5-LO inhibitory activity ranges gave encouraging performances with a satisfactory prediction rate of 46% (11/24).

Fifteen out of these 24 compounds exhibited experimental IC₅₀ values below 300 nM, which confirmed the importance of the carbonyl for 5-LO inhibition by GA analogues. This finding could be explained through an H-bond interaction between the carbonyl group and the amide function of Val110 (Figure 1 and 3).

The docking results showed a π-π interaction between the phenyl moiety of **4** and the imidazole of His130 leading to a higher affinity of **4** in comparison to the corresponding cyclohexyl analogue **11** (Figure 3). It was validated by biological data for **4** and **11** in the δ-series (IC₅₀ (**4**) = 50 ± 23 nM vs IC₅₀ (**11**) = 129 ± 25 nM), and similarly for the analogues in the α- and β-series (IC₅₀ (**12**) = 595 ± 208 nM vs IC₅₀ (**19**) = 998 ± 157 nM, and IC₅₀ (**20**) = 538 ± 107 nM vs IC₅₀ (**27**) > 1000 nM – Table 1).

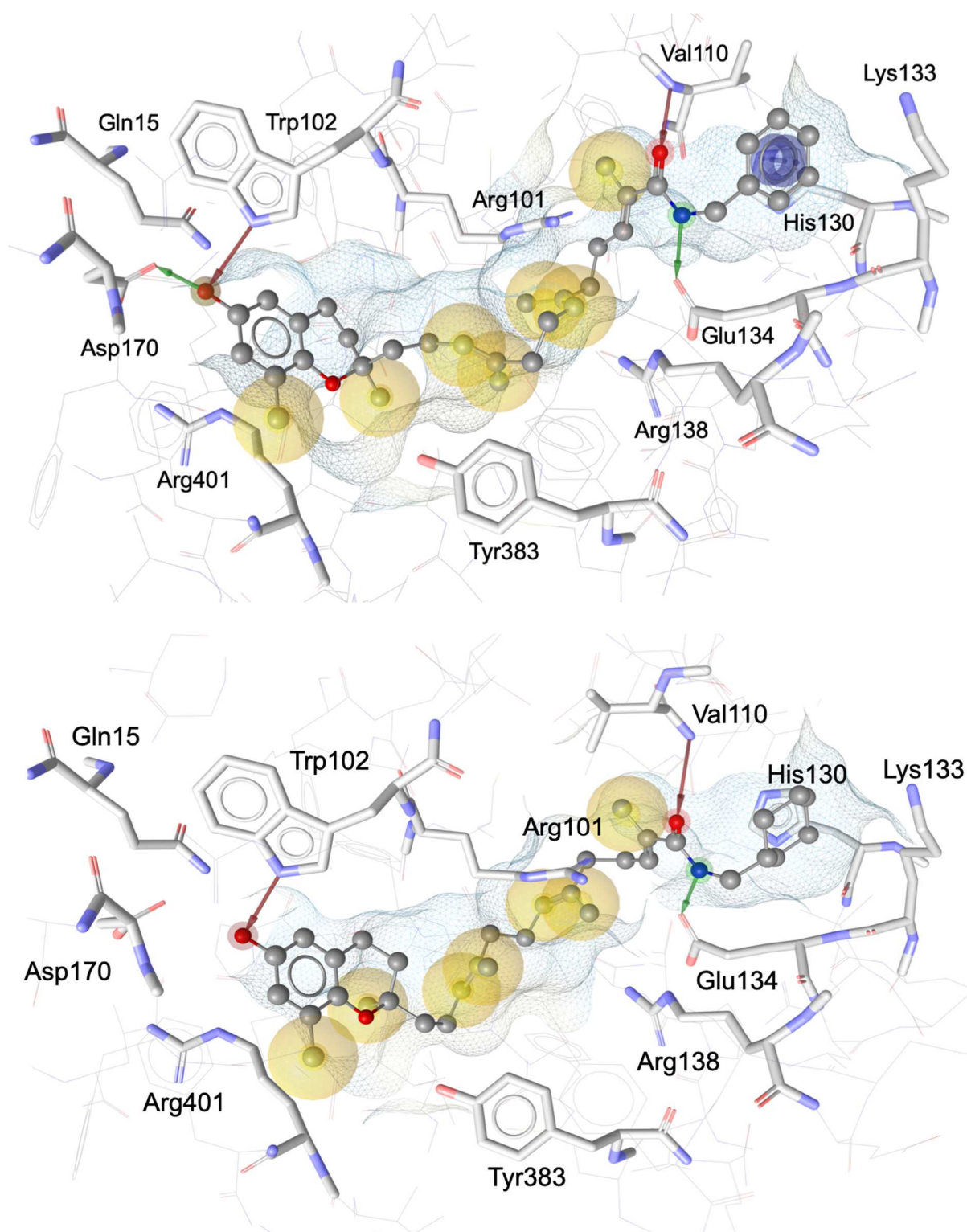


Figure 3: The best-docked pose of compound **4** (above) and **11** (below). Hydrogen bonds are shown as red and green arrows, hydrophobic contacts as yellow spheres, and π - π interaction as blue circle.

Interestingly, the pyridyl derivative **6** had a similar IC_{50} value than **4** (77 ± 6 and 50 ± 23 nM respectively) while the heterocyclic amides **14** and **22** of the α - and β -series were slightly more active than the respective carbocyclic amides **12** and **20**. This discrepancy between different methyl substitution patterns of the chromanol could be explained by steric clashes of

additional methyl groups on this ring leading to a loss of H-bond between the phenol function and the indole of Trp102. Consequently, the ligands **14** and **22** shifted toward Lys133 creating a new favourable H-bond between the pyridyl nitrogen and the primary amine function of Lys133 (Figure 4).

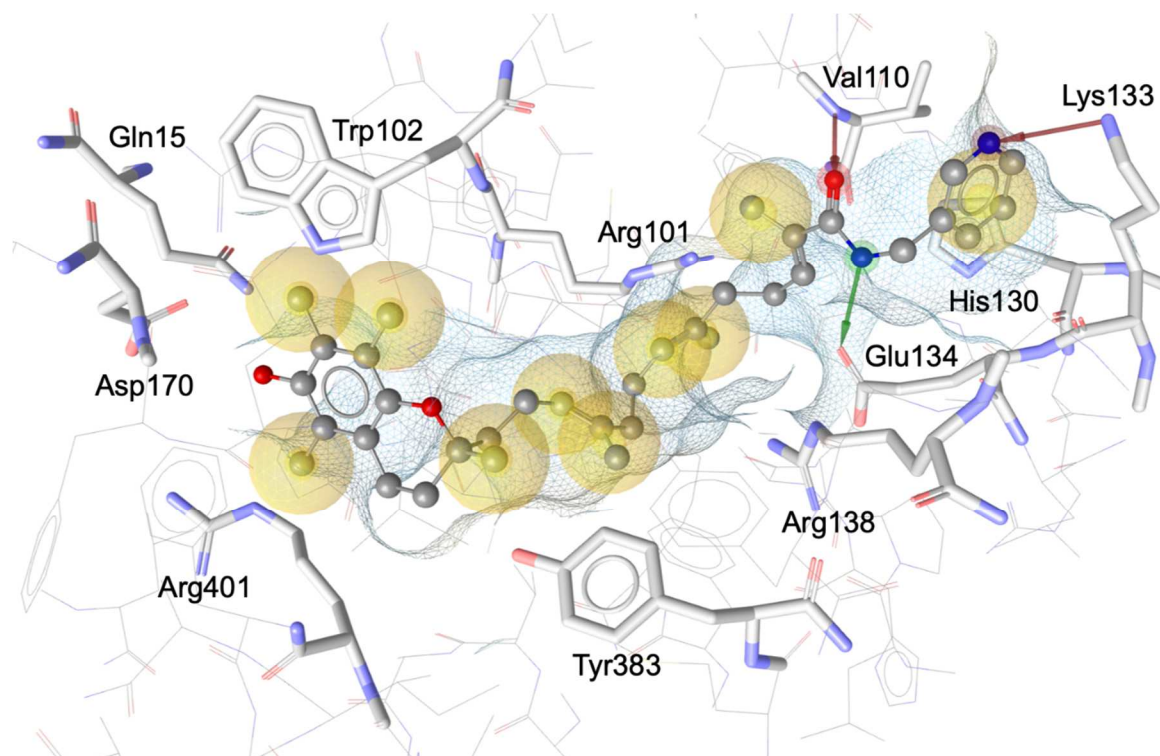


Figure 4: The best-docked pose of compound **14**. Hydrogen bonds are shown as red and green arrows, hydrophobic contacts as yellow spheres.

The substitution of the phenyl moiety with a methoxy group was then examined at *ortho*- (**7**, **15**, **23**), *meta*- (**8**, **16**, **24**), and *para*- (**9**, **17**, **25**) positions. Independent of the position of the alkoxy group, the inhibitory activity remained close to that of the non-substituted phenyl derivatives in the α - and δ -series (**4**, **12**), whereas the corresponding β -garcinamides **23**, **24** and **25** were 4-fold more active than **20**.

The H-bond interaction between the NH of garcinamides and Glu134 was regularly observed. In order to investigate the importance of this structural parameter, tertiary amides **5**, **13** and **21** were docked, semi-synthesized and evaluated. The docked poses of these molecules showed a high variability of conformations in terms of position within the binding site and interactions with crucial residues. Consequently, the model led to predictions of IC₅₀ values with a different level of confidence. Thus, despite a satisfactory correlation between *in silico* and biological results for amide **21**, compound **5** was eventually more active than predicted. Nevertheless, biological results pointed out that these *N,N*-benzylethylamides **5** and **13** were as active as the corresponding benzylamides **4** and **12** while the IC₅₀ of **21** was slightly lower than that of **20**. Hence, the H-bond between the NH of garcinamides and

Glu134 was not crucial for the inhibitory activity as its loss might be compensated by alternative hydrophobic interactions involving the *N*-ethyl group. This hypothesis could not be supported by docking studies because of the high variability of conformations previously mentioned. The same trend was observed also for the other set of tertiary amides **10**, **18**, and **26** that exhibited IC₅₀ values ranging from 131 ± 17 to 265 ± 13 nM.

All garcinamides were additionally evaluated for inhibition of 5-LO in intact human PMNL, a cell-based assay which takes different cellular uptake/retention efficacies into account. Benzylamide **12** (α -series) was 10-fold more active than α -GA while the other benzylamides **4** (δ -series) and **20** (β -series) were as active as δ - and β -GA, respectively. On the other hand, cyclohexyl analogues **11**, **19** and **27** were all inactive (IC₅₀ > 3000 nM). These results highlighted that the phenyl ring is not only favourable for 5-LO inhibition but also for providing access to the cellular target site. Replacing this ring with a 3-pyridyl did not improve the potency of the corresponding analogues (**6**, **14**, and **22**). The *ortho*- and *meta*-substitution of the phenyl ring with a methoxy group was detrimental as the resulting amides in all series (δ , α , and β) were inactive. However, the presence of *para*-methoxy substituent was tolerated with amides **9** and **17**, yielding 2-fold and 6-fold more active derivatives than the parent GA, respectively. Most of δ -garcinamides (**4** – **11**) were comparably active (187 nM < IC₅₀ < 561 nM) to the reference δ -GA **1** (IC₅₀ = 345 ± 73 nM) in PMNL. Note that both reference **1** and compounds **4** – **11** of the δ -series are substantially less potent in the cell-based as compared to the cell-free assay. This trend was not found with α -garcinamides (**12** – **19**), as six out of eight compounds from this series exhibited comparable inhibitory activity in both assays. This suggests superior cellular uptake, retention, subcellular distribution to target sites (nuclear membranes), and/or stability of α -series derivatives.

Lipoxygenase isoenzymes are involved in the metabolism of AA and other polyunsaturated fatty acids leading not only to pro- but also anti-inflammatory lipid mediators (e.g., lipoxins and resolvins). In the current study, we analysed formation of 15-H(P)ETE, a 15-LO-derived precursor of specialized pro-resolving lipid mediators, which actively terminate the inflammatory reaction and promote pathogen clearance and tissue remodelling [27]. Interestingly, most garcinamides led to an increased formation of 15-HETE (Figure 5) [28]. Whether this effect resulted from a specific activation of 15-LO product biosynthesis or simply from substrate channelling from 5-LO to 15-LO needs further investigations. Such complementary study may also explore the consequences on *in vivo* levels of specialized pro-resolving lipid mediators during the resolving phase of inflammation.

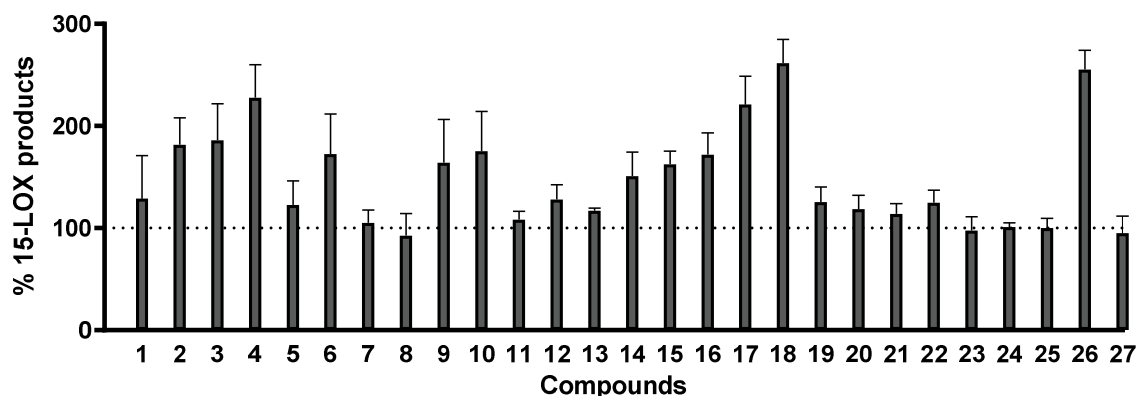


Figure 5: Percentage of 15-LO products formed by activated PMNL in the presence of garcinoic acid isoforms (**1**, **2** and **3**) or garcinamides (**4** – **27**), as compared to vehicle (DMSO) control (100%). Data were expressed as means \pm SEM, $n = 3 - 4$. P values vs vehicle lower than 0.0001 (Student's t -test) were obtained for all 27 compounds.

III. Conclusion

Here, we developed a docking-based semi-quantitative predictive model to rationalize the design of vitamin E derivatives as 5-LO inhibitors. A training set of 17 compounds previously evaluated as 5-LO inhibitors was used to build the model exhibiting a satisfactory correlation between calculated and measured pIC_{50} with $R^2 = 0.86$. A virtual library of 117 garcinamides was screened. Among them, 24 derivatives were selected, semi-synthesized, and biologically evaluated. The comparison between calculated and measured pIC_{50} proved the accuracy of the model with a success rate of 46%. Hence, this study highlighted novel important structural features of an allosteric inhibitor binding site of 5-LO, involving e.g. Val110, His130, Glu134. It also allowed to explore further the chemical space for GA analogues and to identify three new active garcinamides (**9**, **12**, **17**) from the α - and δ -series bearing either a N -benzyl or a N -4-methoxybenzyl moiety. These amides exhibited a significant 5-LO inhibitory activity in both cell-free and cell-based assays. They are promising candidates for further pre-clinical development, with potentially superior stability and bioavailability as compared to the parent long-chain aliphatic acids. Moreover, the strategy reported here promises straightforward *in silico* design for other series of oxidized vitamin E analogues targeting 5-LO.

IV. Experimental section

1. Molecular docking

The molecular docking simulation was conducted with GOLD 5.6.3 (CCDC, Cambridge, UK) [20]. The built-in CHEMPLP scoring function was used to rescore the outputted poses (10 best-scored poses were kept for each compound). The stable crystallographic tri-dimensional

structure of 5-LO was downloaded from the Protein Data Bank (PDB entry 3O8Y) [29][30]. Four *in silico* mutations were inserted in order to return to the 5-LO wild-type sequence: E13W, H14F, G75W, and S76L. The residues were exchanged and the structure was energetically minimized in Discovery Studio 3.5 (Biovia, San Diego, CA) [31]. Hydrogen atoms were added with GOLD, using default settings. The binding site was constituted by 11 amino acid residues: Gln15, Arg101, Tyr81, Tyr100, Arg101, Trp102, Val110, Glu134, Asp170, Arg401 and Glu622. Hydrogen-bond constraints were applied to Trp102-H ϵ 1, Val110-HN, Glu134-O ϵ 1, Asp170-O δ 1, Arg401-HH2, and Arg401-H ϵ with the constraint weight varying from 7 to 40 and the minimum H-bond geometry weight at 0.005. The ligands were allowed to detect internal H-bonds, flip pyramidal N, and flip amide bonds. The correlation as well as the linear regression equation between the calculated pIC₅₀, converted from fitness score, and the measured pIC₅₀ values was computed using Graphpad Prism 8.3.0. Protein-ligand interactions of docking poses were analyzed using LigandScout 4.3 (Inteligand, Vienna, AT) [32].

2. Semi-synthesis

General experimental procedures: all solvents were dried and distilled before use. Reaction were performed in an inert nitrogen atmosphere. Unless otherwise stated, materials purchased from commercial suppliers were used without further purification. Ultrasound-assisted extraction was performed on hundred-gram scale with a PEX03 Sonifier (REUS, Contes, France). Reactions under microwave irradiation were performed in a Monowave 300 (Anton Paar), equipped with the MAS 24 autosampler, using borosilicate glass vials with snap caps. IR spectra were recorded on a Thermo Scientific Nicolet iS5 ATR-FTIR spectrometer and are reported in terms of frequency of absorption (cm⁻¹). ¹H-NMR and ¹³C-NMR spectra were recorded on a JEOL 400 MHz NMR spectrometer in deuterated solvents and calibrated using the residual undeuterated solvent resonance as internal reference. Chemical shifts δ are given in ppm and coupling constants J in Hz. Mass spectrometry analyses were performed on a JMS-700 (JEOL) double-focusing mass spectrometer with reversed geometry, equipped with a pneumatically assisted ESI source. Column chromatography was performed by using silica gel 60 Å (particle size 40–63 μ m) from Fisher Scientific. Flash chromatography purifications using prepacked columns (silica, 4 to 330 g) were carried out on a CombiFlash R_f-200 apparatus equipped with a gradient pump, a column station with a DASi introduction system, a multiwavelength UV detector, a fraction collector, and appropriate software to control the device. HPLC analyses were performed with a Waters Alliance HPLC system (Milford, CT, USA) equipped with a quaternary HPLC pump, degasser, autosampler, and UV detector.

Plant material: *G. kola* nuts were purchased from RIVEX SARL, Angers, France, in January 2016. Plant identification was verified by one of the authors (P.R.). A voucher specimen (GK201601) was deposited at the SONAS laboratory, University of Angers.

Extraction and purification of δ -GA (**1**):

The extraction, purification and identification of δ -GA were achieved following the procedure previously published [23].

Semi-synthesis of α -GA (**2**):

(2*E*,6*E*,10*E*)-13-((*R*)-6-hydroxy-2,5,7,8-tetramethylchroman-2-yl)-2,6,10-trimethyltrideca-2,6,10-trienoic acid (**2**): To a solution of δ -GA (**1**) (400 mg, 0.94 mmol, 1 eq) in dioxane (14 mL), TMDA (2.56 mL, 18.80 mmol, 20 eq) and paraformaldehyde (569 mg, 18.80 mmol, 20 eq) were added. The reaction mixture was heated at 140 °C for 20 min under microwave irradiation. After cooling to room temperature, the solvent was evaporated to dryness. The crude product was dissolved in ethanol (14 mL), and treated with NaBH₃CN (1772 mg, 28.20 mmol, 30 eq). The reaction mixture was heated under reflux for 14 h. Then it was acidified to pH 1 by adding HCl 1N and was extracted with diethyl ether (3 x 100 mL). The combined organic layers were washed with water (2 x 100 mL), brine (100 mL) then dried over Na₂SO₄, and evaporated to dryness. The crude product was purified by flash column chromatography on silica gel, eluting with petroleum ether/acetone (9:1) mixture to afford the desired product as a light-yellow oil (343 mg, 80% yield); *R*_f = 0.45 (DCM/MeOH 9:1); ¹H NMR (400 MHz, CDCl₃) δ 6.87 (td, *J* = 7.2, 1.0 Hz, 1H), 5.13 (t, *J* = 6.6 Hz, 2H), 2.61 (t, *J* = 6.8 Hz, 2H), 2.28 (dd, *J* = 14.9, 7.4 Hz, 2H), 2.16 – 1.95 (m, 17H), 1.83 – 1.73 (m, 5H), 1.67 – 1.49 (m, 8H), 1.25 (s, 3H); ¹³C NMR (100 MHz, CDCl₃) δ 172.7, 145.6, 145.0, 144.7, 135.0, 133.8, 126.9, 125.4, 124.7, 122.8, 121.2, 118.6, 117.5, 74.4, 39.7, 39.6, 38.2, 31.7, 27.7, 26.7, 23.9, 22.3, 20.9, 16.1, 16.0, 12.4, 12.2, 11.9, 11.4; HRMS (FAB) *m/z* calcd for C₂₉H₄₂O₄ [M]⁺ 454.3078, found 454.3084; IR (neat) ν_{max} 3489, 2965, 2851, 1680, 1452, 1240, 927 cm⁻¹.

Semi-synthesis of β -GA (**3**):

(2*E*,6*E*,10*E*)-13-((*R*)-6-hydroxy-2,5,8-trimethylchroman-2-yl)-2,6,10-trimethyltrideca-2,6,10-trienoic acid (**3**): To a solution of δ -GA (**1**) (396 mg, 0.93 mmol, 1 eq) in ethanol (12 mL), TMDA (0.38 mL, 2.79 mmol, 3 eq) and paraformaldehyde (84 mg, 2.79 mmol, 3 eq) were added. The reaction mixture was heated at 120 °C for 20 min under microwave irradiation. Then NaBH₃CN (468 mg, 7.44 mmol, 8 eq) was added and the reaction mixture was heated under reflux for 14 h. It was acidified to pH 1 with HCl 1N and was extracted with diethyl ether (3 x 100 mL). The combined organic layers were washed with water (2 x 100 mL), brine (100 mL) then dried over Na₂SO₄, and evaporated to dryness. The crude product was

purified by flash chromatography column on silica gel, eluting with petroleum ether/acetone mixture to afford the desired product as a yellow oil (261 mg, 64% yield); R_f = 0.45 (DCM/MeOH 9:1); ^1H NMR (400 MHz, CDCl_3) δ 6.88 (td, J = 7.2, 1.1 Hz, 1H), 6.48 (s, 1H), 5.13 (t, J = 6.7 Hz, 2H), 2.61 (t, J = 6.8 Hz, 2H), 2.28 (dd, J = 14.9, 7.2 Hz, 2H), 2.16 – 1.95 (m, 14H), 1.87 – 1.74 (m, 5H), 1.66 – 1.48 (m, 8H), 1.25 (s, 3H); ^{13}C NMR (101 MHz, CDCl_3) δ 173.1, 146.0, 145.8, 145.1, 135.0, 133.8, 127.0, 125.3, 124.6, 124.2, 120.4, 119.3, 115.5, 74.4, 39.7, 39.4, 38.2, 31.6, 27.7, 26.6, 23.9, 22.3, 20.9, 16.1, 16.0 (2C), 12.2, 11.1; HRMS (FAB) m/z calcd for $\text{C}_{28}\text{H}_{40}\text{O}_4$ $[\text{M}]^+$ 440.2921, found 440.2917; IR (neat) ν_{max} 3397, 2922, 2581, 1682, 1641, 1414, 1229, 915 cm^{-1} .

General procedure for amide synthesis from GA isoforms:

To a stirred solution of GA isoform (α , β or δ) (0.12 mmol) in DMF (3 mL) were added an appropriate amine derivative (0.18 mmol, 1.5 eq), diisopropylethylamine (0.36 mmol, 3 eq) and HBTU (0.18 mmol, 1.5 eq). The reaction mixture was stirred at room temperature for 18 h. Then the reaction was quenched with water (1 mL). The resulting mixture was extracted with diethyl ether (3 x 20 mL). The combined organic layers were washed with water (2 x 20 mL), brine (20 mL) then dried over Na_2SO_4 , and evaporated to dryness. The crude product was purified either by reverse-phase flash column chromatography, eluting with water/MeOH (50:50 to 0:100) mixture or by flash column chromatography eluting with PE/Acetone (80:20 to 60:40) mixture to afford the desired product.

(2*E*,6*E*,10*E*)-*N*-benzyl-13-((*R*)-6-hydroxy-2,8-dimethylchroman-2-yl)-2,6,10-trimethyltrideca-2,6,10-trienamide (**4**): δ -GA **1** reacted with benzylamine to give product **4** (88% yield) as a brown oil; R_f = 0.26 (PE/acetone 8:2); ^1H NMR (400 MHz, CDCl_3) δ 7.36 – 7.28 (m, 5H), 6.50 (d, J = 2.6 Hz, 1H), 6.40 (d, J = 2.7 Hz, 1H), 6.36 (t, J = 7.2 Hz, 1H), 6.08 (t, J = 5.1 Hz, 1H, NH), 5.96 (s, 1H, OH), 5.09 (q, J = 6.2 Hz, 2H), 4.51 (d, J = 5.6 Hz, 2H), 2.67 (t, J = 6.7 Hz, 2H), 2.19 (dd, J = 7.4, 15.0 Hz, 2H), 2.11 – 1.94 (m, 11H), 1.85 – 1.69 (m, 5H), 1.65 – 1.48 (m, 8H), 1.27 (s, 3H); ^{13}C NMR (100 MHz, CDCl_3) δ 169.7, 148.5, 145.6, 138.4, 136.8, 134.8, 134.1, 130.5, 128.9 (2C), 128.0 (2C), 127.6, 127.2, 125.0, 124.7, 121.2, 115.9, 112.8, 75.3, 44.0, 39.6, 39.2, 38.5, 31.5, 27.2, 26.5, 24.4, 22.6, 22.3, 16.2, 16.1, 15.9, 12.9; HRMS (FAB) m/z calcd for $\text{C}_{34}\text{H}_{45}\text{NO}_3$ $[\text{M}]^+$ 515.3399, found 515.3387; IR (neat) ν_{max} 3328, 2924, 2850, 2360, 2342, 1659, 1617, 1528, 1469, 1219, 933, 698 cm^{-1} .

(2*E*,6*E*,10*E*)-*N*-benzyl-*N*-ethyl-13-((*R*)-6-hydroxy-2,8-dimethylchroman-2-yl)-2,6,10-trimethyltrideca-2,6,10-trienamide (**5**): δ -GA **1** reacted with *N*-benzylethanamine to give product **5** (60% yield) as a brown oil; R_f = 0.34 (PE/acetone 8:2); ^1H NMR (400 MHz, CDCl_3) δ 7.35 – 7.22 (m, 5H), 6.48 (d, J = 2.9 Hz, 1H), 6.38 (d, J = 2.9 Hz, 1H), 5.53 (td, J = 7.2, 1.5 Hz, 1H), 5.06 (t, J = 6.8 Hz, 2H), 4.60 (s, 2H), 3.30 (s, 2H), 2.67 (t, J = 6.8 Hz, 2H), 2.11 –

1.94 (m, 13H), 1.85 – 1.70 (m, 5H), 1.63 – 1.45 (m, 8H), 1.28 (s, 3H), 1.09 (t, $J = 7.1$ Hz, 3H); ^{13}C NMR (100 MHz, CDCl_3) δ 174.6, 148.5, 145.6, 134.6, 134.4, 131.3 (2C), 128.8 (4C), 127.5, 127.2, 124.9, 124.7 (2C), 121.1, 115.9, 112.8, 75.3, 39.4, 38.7, 38.6, 31.6, 26.3 (2C), 24.8, 22.6, 22.3, 16.2, 16.1, 15.9, 14.7; HRMS (EI) m/z calcd for $\text{C}_{36}\text{H}_{49}\text{NO}_3$ $[\text{M}]^+$ 543.3712 found 543.3703; IR (neat) ν_{max} 3316, 2924, 2852, 1780, 1601, 1472, 1453, 2=1433, 1377, 1220, 743, 698 cm^{-1} .

(2*E*,6*E*,10*E*)-13-(6-hydroxy-2,8-dimethylchroman-2-yl)-2,6,10-trimethyl-*N*-(pyridin-3-ylmethyl)trideca-2,6,10-trienamide (**6**): δ -GA **1** was reacted with pyridin-3-ylmethanamine to give product **6** (65% yield) as a brown oil; $R_f = 0.59$ (PE/acetone 6:4); ^1H NMR (400 MHz, CDCl_3) δ 8.54 (d, $J = 12.7$ Hz, 2H), 7.71 (d, $J = 7.8$ Hz, 1H), 7.30 (t, $J = 6.9$ Hz, 1H), 6.48 (d, $J = 2.6$ Hz, 1H), 6.38 (d, $J = 2.6$ Hz, 1H), 6.35 (t, $J = 6.7$ Hz, 1H), 6.18 (t, $J = 5.4$ Hz, 1H), 5.09-5.06 (m, 2H), 4.53 (d, $J = 5.9$ Hz, 2H), 2.66 (t, $J = 6.8$ Hz, 2H), 2.21 – 2.16 (m, 2H), 2.10 (s, 3H), 2.09 – 1.95 (m, 8H), 1.84 – 1.71 (m, 5H), 1.56 (s, 6H), 1.65 – 1.50 (m, 2H), 1.27 (s, 3H); ^{13}C NMR (100 MHz, CDCl_3) δ 169.7, 148.6, 148.5, 148.4, 145.7, 137.1, 136.5, 134.7, 134.1, 130.3, 127.3, 125.0 (2C), 124.0 (2C), 121.3, 116.0, 112.8, 75.4, 41.3, 39.5, 38.9, 38.6, 31.6, 27.3, 26.2, 24.7, 22.6, 22.3, 16.2, 16.1, 15.9, 12.9; HRMS (EI) m/z calcd for $\text{C}_{33}\text{H}_{44}\text{N}_2\text{O}_3$ $[\text{M}]^+$ 516.3352 found 516.3347; IR (neat) ν_{max} 3316, 2923, 2851, 1659, 1617, 1525, 1470, 1430, 1298, 1260, 1150, 1014, 793 cm^{-1} .

(2*E*,6*E*,10*E*)-13-((*R*)-6-hydroxy-2,8-dimethylchroman-2-yl)-*N*-(2-methoxybenzyl)-2,6,10-trimethyltrideca-2,6,10-trienamide (**7**): δ -GA **1** reacted with (2-methoxyphenyl)methanamine to give product **7** (35% yield) as a brown oil; $R_f = 0.86$ (PE/acetone/DCM 7:2:1); ^1H NMR (400 MHz, CDCl_3) δ 7.26 (td, $J = 10.1, 7.6$ Hz, 2H), 6.89 (dd, $J = 17.7, 7.8$ Hz, 2H), 6.50 (d, $J = 2.6$ Hz, 1H), 6.40 (d, $J = 2.6$ Hz, 1H), 6.32 (t, $J = 6.4$ Hz, 2H), 5.08 (q, $J = 6.8$ Hz, 2H), 4.50 (d, $J = 5.8$ Hz, 2H), 3.84 (s, 3H), 2.65 (t, $J = 6.8$ Hz, 2H), 2.16 (q, $J = 7.6, 6.3$ Hz, 2H), 2.10 – 1.92 (m, 11H), 1.81 – 1.67 (m, 5H), 1.64 – 1.46 (m, 8H), 1.25 (s, 3H); ^{13}C NMR (100 MHz, CDCl_3) δ 169.5, 157.7, 148.6, 145.5, 136.5, 134.8, 134.2, 130.6, 130.0, 129.0, 127.1, 126.3, 124.9, 124.7, 121.1, 120.9, 115.9, 112.8, 110.4, 75.2, 55.4, 39.9, 39.6, 39.2, 38.5, 31.6, 27.2, 26.5, 24.4, 22.6, 22.3, 16.2, 16.1, 15.9, 12.8. HRMS (EI) m/z calcd for $\text{C}_{35}\text{H}_{47}\text{NO}_4$ $[\text{M}]^+$ 545.3505 found 545.3503. IR (neat) ν_{max} 3331, 2924, 1660, 1603, 1464, 1242, 1219, 855, 752 cm^{-1} .

(2*E*,6*E*,10*E*)-13-((*R*)-6-hydroxy-2,8-dimethylchroman-2-yl)-*N*-(3-methoxybenzyl)-2,6,10-trimethyltrideca-2,6,10-trienamide (**8**): δ -GA **1** reacted with (3-methoxyphenyl)methanamine to give product **8** (37% yield) as a brown oil; $R_f = 0.23$ (PE/acetone 8:2); ^1H NMR (400 MHz, CDCl_3) δ 7.25 (t, $J = 7.8$ Hz, 1H), 6.85 (dd, $J = 22.4, 8.2$ Hz, 3H), 6.49 (d, $J = 2.6$ Hz, 1H), 6.40 (d, $J = 2.7$ Hz, 1H), 6.36 (t, $J = 7.3$ Hz, 1H), 6.07 (t, $J = 5.1$ Hz, 1H), 5.09 (q, $J = 6.0$ Hz, 2H), 4.49 (d, $J = 5.6$ Hz, 2H), 3.79 (s, 3H), 2.66 (t, $J = 6.8$ Hz, 1H), 2.19 (dd, $J = 15.2, 7.4$ Hz,

2H), 2.11 – 1.94 (m, 11H), 1.85 – 1.69 (m, 5H), 1.65 – 1.47 (m, 2H), 1.65 (s, 6H), 1.25, (s, 3H); ^{13}C NMR (100 MHz, CDCl_3) δ 169.7, 159.9, 148.4, 145.6, 140.0, 136.9, 134.8, 134.2, 130.4, 129.9, 127.2, 124.9, 124.7, 121.2, 120.2, 115.9, 113.6, 113.0, 112.8, 75.3, 55.3, 44.0, 39.6, 39.2, 38.5, 31.5, 27.2, 26.4, 24.5, 22.6, 22.3, 16.2, 16.1, 15.9, 12.9; HRMS (EI) m/z calcd for $\text{C}_{35}\text{H}_{47}\text{NO}_4$ $[\text{M}]^+$ 545.3505 found 545.3499; IR (neat) ν_{max} 3322, 2922, 2850, 1659, 1601, 1526, 1465, 1435, 1263, 1218, 1147, 1047, 854 cm^{-1} .

(2*E*,6*E*,10*E*)-13-((*R*)-6-hydroxy-2,8-dimethylchroman-2-yl)-*N*-(4-methoxybenzyl)-2,6,10-trimethyltrideca-2,6,10-trienamide (**9**): δ -GA **1** reacted with (4-methoxyphenyl)methanamine to give product **9** (98% yield) as a brown oil; R_f = 0.25 (PE/acetone 7:3); ^1H NMR (400 MHz, CDCl_3) δ 7.23 (d, J = 8.7 Hz, 2H), 6.87 (d, J = 8.7 Hz, 2H), 6.48 (d, J = 2.7 Hz, 1H), 6.39 (d, J = 2.7 Hz, 1H), 6.34 (t, J = 7.2 Hz, 1H), 5.95 (t, J = 5.0 Hz, 1H), 5.08 (q, J = 6.9 Hz, 2H), 4.44 (d, J = 5.6 Hz, 2H), 3.79 (s, 3H), 2.67 (t, J = 6.8 Hz, 2H), 2.20 – 2.15 (m, 2H), 2.11 (s, 3H), 2.10 – 1.93 (m, 8H), 1.83 – 1.66 (m, 5H), 1.66 – 1.47 (m, 8H), 1.27 (s, 3H); ^{13}C NMR (100 MHz, CDCl_3) δ 169.6, 159.1, 148.3, 145.7, 136.7, 134.8, 134.2, 130.5 (2C), 129.4 (2C), 127.3, 124.9, 124.8, 121.2, 115.9, 114.2 (2C), 112.8, 75.3, 55.4, 43.5, 39.6, 39.1, 38.5, 31.5, 27.2, 26.4, 24.5, 22.6, 22.3, 16.2, 16.1, 15.9, 12.9; HRMS (EI) m/z calcd for $\text{C}_{35}\text{H}_{47}\text{NO}_4$ $[\text{M}]^+$ 545.3505 found 545.3503; IR (neat) ν_{max} 3321, 2923, 2851, 1658, 1612, 1512, 1465, 1246, 1218, 1175, 1034, 753 cm^{-1} .

(2*E*,6*E*,10*E*)-13-((*R*)-6-hydroxy-2,8-dimethylchroman-2-yl)-2,6,10-trimethyl-1-(piperidin-1-yl)trideca-2,6,10-trien-1-one (**10**): δ -GA **1** reacted with piperidine to give product **10** (71% yield) as a brown oil; R_f = 0.50 (PE/acetone 7:3); ^1H NMR (400 MHz, acetone- d_6) δ 6.45 (d, J = 2.5 Hz, 1H), 6.35 (d, J = 2.5 Hz, 1H), 5.41 (td, J = 7.1, 1.5 Hz, 1H), 5.14 (q, J = 7.2 Hz, 2H), 3.47 – 3.45 (m, 4H), 2.67 (t, J = 6.9 Hz, 2H), 2.21 – 2.09 (m, 6H), 2.07 (s, 3H), 2.00 – 1.97 (m, 2H), 1.84 – 1.70 (m, 5H), 1.65 – 1.52 (m, 10H), 1.52 – 1.46 (m, 4H), 1.25 (s, 3H); ^{13}C NMR (100 MHz, acetone- d_6) δ 172.3, 150.7, 145.8, 135.4, 135.2, 132.6, 130.1, 127.2, 125.7, 125.6, 121.8, 116.6, 113.5, 75.8, 40.4, 40.1, 39.5, 32.3, 27.2, 27.1, 27.0, 26.7, 25.5 (2C), 24.6 (2C), 23.1, 23.0, 16.4, 16.1, 16.0, 14.7; HRMS (EI) m/z calcd for $\text{C}_{32}\text{H}_{47}\text{NO}_3$ $[\text{M}]^+$ 493.3559 found 493.3553; IR (neat) ν_{max} 2935, 2854, 1593, 1470, 1443, 1216, 853, 749 cm^{-1} .

(2*E*,6*E*,10*E*)-*N*-(cyclohexylmethyl)-13-((*R*)-6-hydroxy-2,8-dimethylchroman-2-yl)-2,6,10-trimethyltrideca-2,6,10-trienamide (**11**): δ -GA **1** reacted with cyclohexanemethylamine to give product **11** (77% yield) as a yellow oil; R_f = 0.87 (PE/acetone/DCM 7:2:1); ^1H NMR (400 MHz, CDCl_3) δ 6.52 (d, J = 2.4 Hz, 1H), 6.42 (d, J = 2.4 Hz, 1H), 6.30 (t, J = 6.7 Hz, 1H), 5.95 (t, J = 5.7 Hz, 1H), 5.10 (q, J = 6.2 Hz, 2H), 3.15 (t, J = 6.4 Hz, 2H), 2.66 (t, J = 6.7 Hz, 2H), 2.18 (q, J = 7.5 Hz, 2H), 2.10 (s, 3H), 2.12 – 1.94 (m, 8H), 1.83 (s, 3H), 1.80 – 1.62 (m, 8H), 1.58 – 1.43 (m, 9H), 1.25 (s, 3H), 1.22 – 1.08 (m, 2H), 0.96 – 0.88 (m, 2H); ^{13}C NMR (100 MHz,

CDCl₃) δ 170.2, 148.8, 145.3, 136.1, 134.8, 134.1, 130.8, 126.9, 124.9, 124.7, 121.0, 115.9, 112.8, 75.1, 46.1, 39.6, 39.3, 38.5, 37.9, 31.5, 30.9 (2C), 27.0, 26.5, 26.4, 25.9 (2C), 24.3, 22.5, 22.2, 16.1, 16.0, 15.9, 12.8; HRMS (FAB) m/z calcd for C₃₄H₅₁NO₃ [M]⁺ 521.3869 found 521.3864; IR (neat) ν_{\max} 3328, 2921, 2849, 1659, 1615, 1533, 1469, 1448, 1219 cm⁻¹.

(2*E*,6*E*,10*E*)-*N*-benzyl-13-((*R*)-6-hydroxy-2,5,7,8-tetramethylchroman-2-yl)-2,6,10-trimethyltrideca-2,6,10-trienamide (**12**): α -GA **2** reacted with benzylamine to give product **12** (39% yield) as a brown oil; R_f = 0.46 (PE/acetone 7:3); ¹H NMR (400 MHz, CDCl₃) δ 7.36 – 7.28 (m, 5H), 6.32 (t, J = 6.7 Hz, 1H), 5.97 (t, J = 5.8 Hz, NH), 5.11 (t, J = 7.2 Hz, 2H), 4.50 (d, J = 5.6 Hz, 2H), 4.35 (br s, 1H, OH), 2.61 (t, J = 6.8 Hz, 2H), 2.24 – 1.93 (m, 19H), 1.85 – 1.73 (m, 5H), 1.65 – 1.49 (m, 8H), 1.25 (s, 3H); ¹³C NMR (100 MHz, CDCl₃) δ 169.4, 145.6, 144.8, 138.6, 136.2, 136.1, 135.0, 134.2, 130.9, 128.9 (2C), 128.0, 127.6, 125.1, 124.7, 122.7, 121.3, 118.8, 117.4, 74.4, 44.0, 39.7, 39.5, 38.6, 31.7, 27.1, 26.7, 24.0, 22.4, 20.9, 16.1, 16.0, 12.9, 12.4, 11.9, 11.5; HRMS (FAB) m/z calcd for C₃₆H₄₉NO₃ [M]⁺ 543.3712, found 543.3716; IR (neat) ν_{\max} 3327, 2922, 2360, 1659, 1619, 1523, 1452, 1252, 1086, 730, 698 cm⁻¹.

(2*E*,6*E*,10*E*)-*N*-benzyl-*N*-ethyl-13-((*R*)-6-hydroxy-2,5,7,8-tetramethylchroman-2-yl)-2,6,10-trimethyltrideca-2,6,10-trienamide (**13**): α -GA **2** reacted with *N*-benzylethanamine to give product **13** (40% yield) as a yellow oil; R_f = 0.54 (PE/acetone 7:3); ¹H NMR (400 MHz, CDCl₃) δ 7.34 – 7.20 (m, 5H), 5.53 (t, J = 7.3 Hz, 1H), 5.09 (d, J = 7.5 Hz, 2H), 4.59 (s, 2H), 4.47 (br s, 1H, OH), 3.31 (s, 2H), 2.61 (t, J = 6.9 Hz, 2H), 2.19 – 1.93 (m, 19H), 1.85 – 1.73 (m, 5H), 1.68 – 1.49 (m, 8H), 1.25 (s, 3H), 1.08 (t, J = 6.9 Hz, 3H); ¹³C NMR (100 MHz, CDCl₃) δ 174.2, 145.5, 144.8, 137.6, 134.9, 134.3, 131.6, 130.0, 128.8 (2C), 127.9, 127.4, 125.0 (2C), 124.6, 122.7, 121.4, 118.8, 117.4, 74.8, 39.7, 39.4, 38.7, 31.7, 29.8, 26.7, 26.2, 24.0, 22.3, 20.9, 16.0 (2C), 14.8, 14.7, 12.4, 12.1, 11.9, 11.5; HRMS (FAB) m/z calcd for C₃₈H₅₃NO₃ [M]⁺ 571.4025 found 571.4031; IR (neat) ν_{\max} 2921, 2360, 1603, 1422, 1377, 1250, 1086, 730, 697 cm⁻¹.

(2*E*,6*E*,10*E*)-13-((*R*)-6-hydroxy-2,5,7,8-tetramethylchroman-2-yl)-2,6,10-trimethyl-*N*-(pyridin-3-ylmethyl)trideca-2,6,10-trienamide (**14**): α -GA **2** reacted with pyridin-3-ylmethanamine to give product **14** (67% yield) as a yellow oil; R_f = 0.17 (PE/acetone 7:3); ¹H NMR (400 MHz, acetone-*d*₆) δ 8.52 (s, 1H, OH), 8.42 (d, J = 3.6 Hz, 1H), 7.68 (d, J = 7.5 Hz, 2H), 7.28 (dd, J = 7.6, 4.8 Hz, 1H), 6.54 (s, 1H, NH), 6.37 (t, J = 6.0 Hz, 1H), 5.14 (s, 2H), 4.46 (d, J = 6.0 Hz, 2H), 2.59 (t, J = 6.8 Hz, 2H), 2.25 – 1.95 (m, 19H), 1.83 – 1.73 (m, 5H), 1.64 – 1.54 (m, 8H), 1.29 (s, 3H); ¹³C NMR (100 MHz, acetone-*d*₆) δ 169.5, 150.1, 149.0, 146.4, 145.9, 136.5, 136.0, 135.8, 135.3, 134.9, 132.0, 125.6 (2C), 124.1, 123.1, 122.5, 120.6, 117.8, 74.7, 41.4, 40.3, 39.9, 39.3, 32.4, 27.7, 27.2, 24.2, 22.9, 21.4, 16.1, 15.9, 12.9, 12.8, 12.1, 11.8; HRMS

(FAB) m/z calcd for $C_{35}H_{48}N_2O_3$ $[M]^+$ 544.3665 found 544.3668; IR (neat) ν_{\max} 3297, 2921, 2852, 1659, 1619, 1525, 1427, 1378, 1253, 1087, 711 cm^{-1} .

(2*E*,6*E*,10*E*)-13-((*R*)-6-hydroxy-2,5,7,8-tetramethylchroman-2-yl)-*N*-(2-methoxybenzyl)-2,6,10-trimethyltrideca-2,6,10-trienamide (**15**): α -GA **2** reacted with (2-methoxyphenyl)methanamine to give product **15** (40% yield) as a yellow oil; R_f = 0.65 (PE/acetone/DCM 7:2:1); ^1H NMR (400 MHz, CDCl_3) δ 7.29 – 7.24 (m, 3H), 6.94 – 6.87 (m, 2H), 6.29 (t, J = 6.7 Hz, 1H), 6.22 (t, J = 6.4 Hz, 1H), 5.11 (d, J = 2.6 Hz, 2H), 4.50 (d, J = 5.8 Hz, 2H), 3.86 (s, 3H), 2.60 (t, J = 6.7 Hz, 2H), 2.21 – 1.93 (m, 19H), 1.82 – 1.74 (m, 5H), 1.66 – 1.50 (m, 8H), 1.25 (s, 3H); ^{13}C NMR (100 MHz, CDCl_3) δ 169.2, 157.7, 145.6, 144.8, 135.8, 135.0, 134.2, 130.9, 130.0, 128.9, 126.6, 125.0, 124.7, 122.7, 121.4, 120.9, 118.8, 117.4, 110.4, 74.4, 55.5, 39.8, 39.7, 39.5, 38.6, 31.7, 27.1, 26.7, 24.0, 22.4, 20.9, 16.1, 16.0, 12.8, 12.4, 11.9, 11.5; HRMS (EI) m/z calcd for $C_{37}H_{51}NO_4$ $[M]^+$ 573.3818 found 573.3815; IR (neat) ν_{\max} 3345, 2921, 2851, 1620, 1519, 1492, 1462, 1243, 1087, 1051, 751 cm^{-1} .

(2*E*,6*E*,10*E*)-13-((*R*)-6-hydroxy-2,5,7,8-tetramethylchroman-2-yl)-*N*-(3-methoxybenzyl)-2,6,10-trimethyltrideca-2,6,10-trienamide (**16**): α -GA **2** reacted with (3-methoxyphenyl)methanamine to give product **16** (23% yield) as a yellow oil; R_f = 0.59 (PE/acetone/DCM 7:2:1); ^1H NMR (400 MHz, CDCl_3) δ 7.25 (t, J = 7.8 Hz, 1H), 6.89 – 6.80 (m, 3H), 6.32 (t, J = 6.7 Hz, 1H), 5.96 (s, 1H, NH), 5.11 (t, J = 6.3 Hz, 2H), 4.48 (d, J = 5.6 Hz, 2H), 4.36 (br s, 1H, OH), 3.80 (s, 3H), 2.61 (t, J = 6.8 Hz, 2H), 2.24 – 1.93 (m, 19H), 1.85 – 1.75 (m, 5H), 1.66 – 1.51 (m, 8H), 1.25 (s, 3H); ^{13}C NMR (100 MHz, CDCl_3) δ 169.4, 160.0, 145.6, 144.7, 140.2, 136.2, 135.0, 134.2, 130.8, 129.9, 125.1, 124.7, 122.7, 121.3, 120.2, 118.8, 117.4, 113.6, 113.0, 74.4, 55.4, 43.9, 39.7, 38.6, 31.7, 27.1, 26.7, 23.9, 22.4, 20.9, 16.1, 16.0, 12.9, 12.4, 11.9, 11.5; HRMS (EI) m/z calcd for $C_{37}H_{51}NO_4$ $[M]^+$ 573.3818 found 573.3816; IR (neat) ν_{\max} 3339, 2924, 2851, 1660, 1611, 1526, 1453, 1437, 1262, 1165, 1087, 737 cm^{-1} .

(2*E*,6*E*,10*E*)-13-((*R*)-6-hydroxy-2,5,7,8-tetramethylchroman-2-yl)-*N*-(4-methoxybenzyl)-2,6,10-trimethyltrideca-2,6,10-trienamide (**17**): α -GA **2** reacted with (4-methoxyphenyl)methanamine to give product **17** (45% yield) as a yellow oil; R_f = 0.56 (PE/acetone/DCM 7:2:1); ^1H NMR (400 MHz, CDCl_3) δ 7.20 (d, J = 8.2 Hz, 2H), 6.84 (d, J = 8.2 Hz, 2H), 6.28 (t, J = 6.0 Hz, 1H), 5.90 (s, 1H), 5.09 (d, J = 4.6 Hz, 2H), 4.40 (d, J = 4.9 Hz, 2H), 3.77 (s, 3H), 2.58 (t, J = 5.7 Hz, 2H), 2.20 – 1.93 (m, 19H), 1.81 – 1.72 (m, 5H), 1.64 – 1.47 (m, 8H), 1.23 (s, 3H); ^{13}C NMR (100 MHz, CDCl_3) δ 169.4, 159.1, 145.5, 144.8, 136.1, 134.9, 134.1, 130.8, 130.7, 129.3 (2C), 125.1, 124.7, 122.7, 121.4, 118.8, 117.4, 114.2 (2C), 74.4, 55.4, 43.4, 39.7, 39.5, 38.6, 31.7, 27.1, 26.7, 23.9, 22.3, 20.9, 16.1, 16.0,

12.9, 12.4, 11.9, 11.4; HRMS (EI) m/z calcd for $C_{37}H_{51}NO_4$ $[M]^+$ 573.3818 found 573.3813; IR (neat) ν_{\max} 3333, 2923, 2851, 1659, 1612, 1512, 1452, 1447, 1086, 1035, 828, 736 cm^{-1} .

(2*E*,6*E*,10*E*)-13-((*R*)-6-hydroxy-2,5,7,8-tetramethylchroman-2-yl)-2,6,10-trimethyl-1-(piperidin-1-yl)trideca-2,6,10-trien-1-one (**18**): α -GA **2** reacted with piperidine to give product **18** (45% yield) as a yellow oil. R_f = 0.62 (PE/acetone/DCM 7:2:1); 1H NMR (400 MHz, $CDCl_3$) δ 5.45 (t, J = 6.7 Hz, 1H), 5.11 (dd, J = 14.8, 7.1 Hz, 2H), 4.56 (br s, 1H, OH), 3.48 (s, 4H), 2.60 (t, J = 6.4 Hz, 2H), 2.15 – 1.94 (m, 19H), 1.86 – 1.74 (m, 5H), 1.64 – 1.53 (m, 14H), 1.25 (s, 3H); ^{13}C NMR (100 MHz, $CDCl_3$) δ 172.6, 145.5, 144.8, 134.9, 134.4, 131.5, 130.2, 124.9, 124.7, 122.6, 121.4, 118.9, 117.3, 74.3, 39.7, 39.4, 38.8, 31.7, 26.7, 26.2 (2C), 24.8 (2C), 24.0 (2C), 22.3, 20.9, 16.0 (3C), 14.5, 12.4, 11.9, 11.5; HRMS (EI) m/z calcd for $C_{34}H_{51}NO_3$ $[M]^+$ 521.3869 found 521.3862; IR (neat) ν_{\max} 3359, 2924, 2854, 1602, 1444, 1273, 1257, 1088 cm^{-1} .

(2*E*,6*E*,10*E*)-*N*-(cyclohexylmethyl)-13-((*R*)-6-hydroxy-2,5,7,8-tetramethylchroman-2-yl)-2,6,10-trimethyltrideca-2,6,10-trienamide (**19**): α -GA **2** reacted with cyclohexanemethylamine to give product **19** (39% yield) as a yellow oil; R_f = 0.75 (PE/acetone/DCM 7:2:1); 1H NMR (400 MHz, $CDCl_3$) δ 6.25 (t, J = 6.6 Hz, 1H), 5.74 (s, 1H, NH), 5.12 (t, J = 6.7 Hz, 2H), 3.14 (t, J = 6.4 Hz, 2H), 2.61 (t, J = 6.8 Hz, 2H), 2.22 – 1.94 (m, 19H), 1.86 – 1.49 (m, 18H), 1.25 – 1.13 (m, 7H), 0.97 – 0.88 (m, 2H); ^{13}C NMR (100 MHz, $CDCl_3$) δ 169.7, 145.6, 144.8, 135.4, 135.0, 134.2, 131.2, 125.1, 124.7, 122.7, 121.3, 118.8, 117.4, 74.4, 46.0, 39.8, 39.5, 38.6, 38.1, 31.7, 31.0 (2C), 27.0, 26.7, 26.5, 26.0 (2C), 23.9, 22.4, 20.9, 16.1, 16.0, 12.9, 12.4, 11.9, 11.5; HRMS (EI) m/z calcd for $C_{36}H_{55}NO_3$ $[M]^+$ 549.4182 found 549.4180; IR (neat) ν_{\max} 3317, 2924, 2851, 1610, 1532, 1449, 1262, 1087, 737 cm^{-1} .

(2*E*,6*E*,10*E*)-*N*-benzyl-13-((*R*)-6-hydroxy-2,5,8-trimethylchroman-2-yl)-2,6,10-trimethyltrideca-2,6,10-trienamide (**20**): β -GA **3** reacted with benzylamine to give product **20** (66% yield) as a yellow oil; R_f = 0.46 (PE/acetone 7:3); 1H NMR (400 MHz, $CDCl_3$) δ 7.36 – 7.28 (m, 5H), 6.48 (s, 1H), 6.33 (t, J = 6.6 Hz, 1H), 5.97 (br s, NH), 5.10 (s, 2H), 4.51 (d, J = 5.5 Hz, 2H), 2.60 (t, J = 6.8 Hz, 2H), 2.20 (q, J = 7.4 Hz, 2H), 2.13 – 1.93 (m, 14H), 1.85 – 1.73 (m, 5H), 1.60 – 1.47 (m, 8H), 1.25 (s, 3H); ^{13}C NMR (100 MHz, $CDCl_3$) δ 169.5, 146.1, 145.8, 138.5, 136.5, 134.9, 134.2, 130.6, 128.9 (2C), 128.0 (2C), 127.7, 125.1, 124.7, 124.0, 120.4, 119.4, 115.5, 74.3, 44.0, 39.7, 39.1, 38.5, 31.6, 27.1, 26.6, 24.2, 22.3, 20.9, 16.1, 16.0 (2C), 12.9, 11.1; HRMS (FAB) m/z calcd for $C_{35}H_{47}NO_3$ $[M]^+$ 529.3556, found 529.3551; IR (neat) ν_{\max} 2923, 2852, 1659, 1619, 1528, 1454, 1415, 1379, 1230, 1165, 698 cm^{-1} .

(2*E*,6*E*,10*E*)-*N*-benzyl-*N*-ethyl-13-((*R*)-6-hydroxy-2,5,8-trimethylchroman-2-yl)-2,6,10-trimethyltrideca-2,6,10-trienamide (**21**): β -GA **3** reacted with *N*-benzylethanamine to give product **21** (48% yield) as a yellow oil; R_f = 0.51 (PE/acetone 7:3); 1H NMR (400 MHz, $CDCl_3$)

δ 7.35 – 7.22 (m, 5H), 6.49 (s, 1H), 5.53 (td, J = 7.1, 1.2 Hz, 1H), 5.17 (br s, OH), 5.08 (t, J = 6.8 Hz, 2H), 4.60 (s, 2H), 3.31 (s, 2H), 2.60 (t, J = 6.5 Hz, 2H), 2.10 – 1.93 (m, 16H), 1.85 – 1.73 (m, 5H), 1.64 – 1.46 (m, 8H), 1.26 (s, 3H), 1.09 (t, J = 7.1 Hz, 3H); ^{13}C NMR (100 MHz, CDCl_3) δ 174.4, 146.3, 145.7, 137.6, 134.8, 134.4, 131.4, 130.2, 128.8 (2C), 128.0, 127.5 (2C), 124.9, 124.8, 123.9, 120.3, 119.5, 115.6, 74.3, 39.6, 38.9, 38.7, 31.6, 29.8, 26.5, 26.2, 24.3, 22.8, 22.3, 20.9, 16.0 (3C), 14.7, 14.3, 11.2; HRMS (FAB) m/z calcd for $\text{C}_{37}\text{H}_{51}\text{NO}_3$ $[\text{M}]^+$ 557.3869 found 557.3863; IR (neat) ν_{max} 2922, 1596, 1414, 1164, 1097, 857, 725, 697 cm^{-1} .

(2*E*,6*E*,10*E*)-13-((*R*)-6-hydroxy-2,5,8-trimethylchroman-2-yl)-2,6,10-trimethyl-*N*-(pyridin-3-ylmethyl)trideca-2,6,10-trienamide (**22**): β -GA **3** reacted with pyridin-3-ylmethanamine to give product **22** (80% yield) as a yellow oil; R_f = 0.14 (PE/acetone 7:3); ^1H NMR (400 MHz, CDCl_3) δ 8.59 (s, 2H), 7.69 (d, J = 7.7 Hz, 1H), 7.31 (s, 1H), 6.49 (s, 1H), 6.34 (td, J = 7.1, 1.7 Hz, 1H), 6.20 (t, J = 6.0 Hz, 1H, NH), 5.08 (s, 2H), 4.53 (d, J = 5.7 Hz, 2H), 2.60 (t, J = 6.8 Hz, 2H), 2.19 (q, J = 7.4 Hz, 2H), 2.12 – 1.93 (m, 14H), 1.84 – 1.73 (m, 5H), 1.64 – 1.46 (m, 8H), 1.25 (s, 3H); ^{13}C NMR (100 MHz, CDCl_3) δ 169.7, 148.8 (2C), 148.4, 146.4, 145.7, 136.9, 136.3, 134.7, 134.1, 130.4, 125.1, 124.8, 123.9 (2C), 120.4, 119.6, 115.6, 74.3, 41.4, 39.6, 39.0, 38.5, 31.6, 27.2, 26.5, 24.3, 22.3, 20.9, 16.1, 16.0 (2C), 12.9, 11.2; HRMS (FAB) m/z calcd for $\text{C}_{34}\text{H}_{46}\text{N}_2\text{O}_3$ $[\text{M}]^+$ 530.3508 found 531.3570; IR (neat) ν_{max} 3305, 2922, 1659, 1619, 1523, 1414, 1229, 854, 734, 710 cm^{-1} .

(2*E*,6*E*,10*E*)-13-((*R*)-6-hydroxy-2,5,8-trimethylchroman-2-yl)-*N*-(2-methoxybenzyl)-2,6,10-trimethyltrideca-2,6,10-trienamide (**23**): β -GA **3** reacted with (2-methoxyphenyl)methanamine to give product **23** (30% yield) as a yellow oil; R_f = 0.78 (PE/acetone/DCM 7:2:1); ^1H NMR (400 MHz, CDCl_3) δ 7.30 – 7.24 (m, 2H), 6.94 – 6.87 (m, 2H), 6.49 (s, 1H), 6.31 (t, J = 6.8 Hz, 1H), 6.26 (t, J = 5.4 Hz, 1H), 5.09 (dd, J = 12.1, 5.9 Hz, 2H), 4.51 (d, J = 5.7 Hz, 2H), 3.86 (s, 3H), 2.60 (t, J = 6.8 Hz, 2H), 2.20 – 1.93 (m, 16H), 1.85 – 1.73 (m, 5H), 1.61 – 1.47 (m, 8H), 1.26 (s, 3H); ^{13}C NMR (100 MHz, CDCl_3) δ 169.4, 157.7, 146.2, 145.7, 136.2, 134.8, 134.2, 130.7, 130.0, 129.0, 126.5, 124.9, 124.7, 123.9, 120.9, 120.3, 119.5, 115.6, 110.5, 74.3, 55.5, 39.8, 39.6, 39.1, 38.6, 31.6, 27.2, 26.6, 24.2, 22.3, 20.9, 16.1, 16.0 (2C), 12.8, 11.1; HRMS (EI) m/z calcd for $\text{C}_{36}\text{H}_{49}\text{NO}_4$ $[\text{M}]^+$ 559.3662 found 559.3656; IR (neat) ν_{max} 3424, 2924, 2851, 1660, 1619, 1604, 1492, 1464, 1414, 1242, 752, 738 cm^{-1} .

(2*E*,6*E*,10*E*)-13-((*R*)-6-hydroxy-2,5,8-trimethylchroman-2-yl)-*N*-(3-methoxybenzyl)-2,6,10-trimethyltrideca-2,6,10-trienamide (**24**): β -GA **3** reacted with (3-methoxyphenyl)methanamine to give product **24** (51% yield) as a yellow oil; R_f = 0.53 (PE/acetone/DCM 7:2:1); ^1H NMR (400 MHz, CDCl_3) δ 7.25 (t, J = 8.0 Hz, 1H), 6.89 – 6.81 (m, 3H), 6.49 (s, 1H), 6.34 (t, J = 6.8 Hz, 1H), 6.02 (t, J = 5.5 Hz, 1H, NH), 5.10 (s, 2H), 4.49 (d, J = 5.6 Hz, 2H), 3.79 (s, 3H), 2.60

(t, J = 6.9 Hz, 2H), 2.23 – 2.17 (m, 2H), 2.13 – 1.93 (m, 14H), 1.87 – 1.73 (m, 5H), 1.65 – 1.47 (m, 8H), 1.26 (s, 3H); ^{13}C NMR (100 MHz, CDCl_3) δ 169.6, 160.0, 146.2, 145.7, 140.1, 136.5, 134.8, 134.1, 130.6, 129.9, 125.0, 124.7, 123.9, 120.3, 120.2, 119.5, 115.5, 113.6, 113.0, 74.3, 55.4, 43.9, 39.6, 39.1, 38.5, 31.6, 27.2, 26.6, 24.1, 22.3, 20.9, 16.1, 16.0 (2C), 12.9, 11.1; HRMS (EI) m/z calcd for $\text{C}_{36}\text{H}_{49}\text{NO}_4$ $[\text{M}]^+$ 559.3662 found 559.3659; IR (neat) ν_{max} 3339, 2921, 2850, 1660, 1602, 1455, 1435, 1414, 1264, 1230, 1165, 696 cm^{-1} .

(2*E*,6*E*,10*E*)-13-((*R*)-6-hydroxy-2,5,8-trimethylchroman-2-yl)-*N*-(4-methoxybenzyl)-2,6,10-trimethyltrideca-2,6,10-trienamide (**25**): β -GA **3** reacted with (4-methoxyphenyl)methanamine to give product **25** (36% yield) as a yellow oil; R_f = 0.50 (PE/acetone/DCM 7:2:1); ^1H NMR (400 MHz, CDCl_3) δ 7.22 (d, J = 7.9 Hz, 2H), 6.87 (d, J = 7.9 Hz, 2H), 6.49 (s, 1H), 6.32 (t, J = 6.8 Hz, 1H), 5.96 (s, 1H, NH), 5.10 (d, J = 6.2 Hz, 2H), 4.44 (d, J = 5.2 Hz, 2H), 3.79 (s, 3H), 2.60 (t, J = 6.6 Hz, 2H), 2.22 – 2.16 (m, 2H), 2.13 – 1.93 (m, 14H), 1.83 – 1.73 (m, 5H), 1.65 – 1.47 (m, 8H), 1.25 (s, 3H); ^{13}C NMR (100 MHz, CDCl_3) δ 169.5, 159.1, 146.2, 145.7, 136.4, 134.8, 134.2, 130.7, 130.6, 129.4 (2C), 125.0, 124.7, 123.9, 120.3, 119.5, 115.6, 114.2 (2C), 74.3, 55.4, 43.5, 39.7, 39.1, 38.5, 31.6, 27.1, 26.6, 24.1, 22.3, 20.9, 16.1, 16.0 (2C), 12.9, 11.1; HRMS (EI) m/z calcd for $\text{C}_{36}\text{H}_{49}\text{NO}_4$ $[\text{M}]^+$ 559.3662 found 559.3658; IR (neat) ν_{max} 3338, 2922, 2850, 1659, 1613, 1512, 1463, 1414, 1247, 1174 cm^{-1} .

(2*E*,6*E*,10*E*)-13-((*R*)-6-hydroxy-2,5,8-trimethylchroman-2-yl)-2,6,10-trimethyl-1-(piperidin-1-yl)trideca-2,6,10-trien-1-one (**26**): β -GA **3** reacted with piperidine to give product **26** (69% yield) as a yellow oil; R_f = 0.59 (PE/acetone/DCM 7:2:1); ^1H NMR (400 MHz, CDCl_3) δ 6.50 (s, 1H), 5.46 (t, J = 6.6 Hz, 1H), 5.12 – 5.06 (m, 2H), 3.47 (s, 4H), 2.59 (t, J = 6.5 Hz, 2H), 2.17 – 1.94 (m, 16H), 1.86 – 1.73 (m, 5H), 1.64 – 1.46 (m, 14H), 1.25 (s, 3H); ^{13}C NMR (100 MHz, CDCl_3) δ 172.8, 146.5, 145.4, 134.8, 134.4, 131.2, 130.4, 124.8, 124.7, 123.7, 120.2, 119.5, 115.6, 74.2, 39.6, 39.0, 38.7, 31.6, 26.6 (2C), 26.1 (2C), 24.7 (2C), 24.1 (2C), 22.3, 20.9, 16.0 (3C), 14.5, 11.1; HRMS (EI) m/z calcd for $\text{C}_{33}\text{H}_{49}\text{NO}_3$ $[\text{M}]^+$ 507.3712 found 507.370; IR (neat) ν_{max} 3312, 2931, 2853, 1596, 1443, 1415, 1229, 854 cm^{-1} .

(2*E*,6*E*,10*E*)-*N*-(cyclohexylmethyl)-13-((*R*)-6-hydroxy-2,5,8-trimethylchroman-2-yl)-2,6,10-trimethyltrideca-2,6,10-trienamide (**27**): β -GA **3** reacted with cyclohexanemethylamine to give product **27** (27% yield) as a yellow oil; R_f = 0.68 (PE/acetone/DCM 7:2:1); ^1H NMR (400 MHz, CDCl_3) δ 6.49 (s, 1H), 6.27 (t, J = 7.6 Hz, 1H), 5.77 (t, J = 4.9 Hz, 1H, NH), 5.10 (d, J = 2.3 Hz, 2H), 3.15 (t, J = 6.4 Hz, 2H), 2.60 (t, J = 6.8 Hz, 2H), 2.21 – 2.15 (m, 2H), 2.13 – 1.94 (m, 14H), 1.85 – 1.42 (m, 20H), 1.25 – 1.13 (m, 5H), 0.97 – 0.88 (m, 2H); ^{13}C NMR (100 MHz, CDCl_3) δ 169.9, 146.2, 145.7, 135.8, 134.8, 134.2, 131.0, 125.0, 124.8, 123.9, 120.3, 119.5, 115.6, 74.3, 46.1, 39.7, 39.1, 38.6, 38.1, 31.6, 31.0 (2C), 27.1, 26.6, 26.5, 26.0 (2C), 24.2,

22.3, 20.9, 16.1, 16.0 (2C), 12.9, 11.2; HRMS (FAB) m/z calcd for $C_{35}H_{53}NO_3$ $[M]^+$ 535.4025 found 535.4018; IR (neat) ν_{\max} 3328, 2922, 2851, 1659, 1619, 1533, 1414, 1230 cm^{-1} .

3. Biological assays

Determination of purified 5-LO activity

The plasmid pT3-5-LO was transformed into *E. coli* BL21 (DE3) cells to express human recombinant 5-LO, which was purified by affinity chromatography using an ATP-agarose column. In brief, *E. coli* was lysed by incubation in 50 mM triethanolamine/HCl at pH 8.0 with EDTA (5 mM), soybean trypsin inhibitor (60 $\mu\text{g/mL}$), 1 mM phenylmethylsulphonyl fluoride, and lysozyme (500 $\mu\text{g/mL}$). After homogenization by sonication (3 x 15 s) and centrifugation (10,000 x g) for 15 min, the supernatant was centrifuged again at 40,000 x g for 70 min at 4 °C. The supernatant was then applied into an ATP-agarose column and the column was washed first with PBS buffer (pH 7.4) plus 1 mM EDTA, then with 50 mM phosphate buffer (pH 7.4) 0.5 M NaCl, 1 mM EDTA, and finally with 50 mM phosphate buffer (pH 7.4). The 5-LO enzyme was eluted with 50 mM phosphate buffer (pH 7.4), 1 mM EDTA, and 20 mM ATP.

Purified 5-LO (0.5 μg) in 1 mL of PBS buffer pH 7.4 containing EDTA (1 mM), and ATP (1 mM) was pre-incubated with test compounds or vehicle control (0.1% DMSO) for 10 min on ice and pre-warmed for 30 s at 37 °C. 5-LO production formation was started at 37 °C by adding 5 μL of AA (20 μM) and 5 μL of CaCl_2 (2 mM). After 10 min of incubation, 1 mL of ice-cold methanol was added and formed 5-LO products (all-trans isomers of LTB_4 and 5-H(P)ETE) were extracted using Sep-Pak C18 35 cc Vac Cartridges (Waters, Milford, MA). 5-LO products were separated by RP-HPLC on a Nova-Pak C18 Radial-Pak column (5 x 100 mm, 4 μm , Waters) under isocratic conditions (73% methanol/27% water/0.007% trifluoroacetic acid) at a flow rate of 1.2 mL/min and detected at 235 and 280 nm. PGB_1 was used as internal standard.

Determination of 5-LO product formation in activated PMNL

Leukocyte concentrates were provided by the Institute for Transfusion Medicine, University Hospital Jena (Germany). The protocols for experiments were approved by the ethical commission of the Friedrich-Schiller-University Jena. Blood was freshly collected from fasted (12 h) adult male and female healthy volunteer, with informed consent. These subjects donated blood every 8 – 12 weeks, had no apparent infection, inflammatory conditions, or current allergic reactions (according to prior physical inspection by a clinician) and had not taken antibiotics or anti-inflammatory drugs for at least 10 days prior to blood donation. Venous blood was centrifuged at 4,000 x g/20 min/20 °C in order to concentrate leukocytes,

which were subjected to centrifugation on lymphocyte separation medium (LSM 1077, GE Healthcare, Freiburg, Germany). PMNL were recovered from the pellet after hypotonic lysis of erythrocytes.

Freshly isolated PMNL (5×10^6 cells) were resuspended in ice-cold PBS buffer plus glucose (1 mg/mL) at 4 °C, and CaCl_2 (10 mM) was added. Suspensions were pre-incubated with test compounds or vehicle control (0.1% DMSO) for 10 min at 37 °C. 5-LO product formation was started by treatment with the Ca^{2+} -ionophore A23187 (2.5 μM) and AA (20 μM). After 10 min of incubation, 1 mL of ice-cold methanol was added and formed 5-LO products (all-*trans* isomers of LTB_4 , 5-H(P)ETE and 12-HETE and 15-HETE) were extracted and analysed as described above.

4. Statistics

Data are expressed as mean \pm S.E.M. IC_{50} values were graphically calculated from averaged measurements at 4 – 5 different concentrations of the compound using GraphPad Prism 8.3.0 (GraphPad software, San Diego, US). Linear regression and correlation between the fitness score and measured pIC_{50}s as well as conversion of the latter score to calculated pIC_{50} values were performed also by GraphPad Prism 8.3.0. Statistical evaluation of data was computed by Excel for Office 365 (Microsoft Corporation, Washington, US). A P value < 0.05 was considered significant.

V. Acknowledgements

The authors thank Ingrid Freuze for HRMS measurements of all molecules and Dimitri Bréard for semi-preparative HPLC assistance. C.P.D. received a PhD grant by the French Ministry of Higher Education, Research and Innovation (MESRI). J.J.H. was supported by MESRI and the French Ministry of Europe and Foreign Affairs through PHC fundings (AMADEUS 2017-18 N°38263PF, PROCOPE 2018-2019 N°40507RB). A.K. was supported by the German Research Council (GRK 1715, KO 4589/7-1) and the German Academic Exchange Service (57389523) paid from the German Federal Ministry of Education and Research. The work by O.W. was funded by the German Research Council (SFB 1278 Polytarget) and by the Free State of Thuringia and the European Social Fund (2016 FGR 0045).

VI. References

- [1] R. Medzhitov, Origin and physiological roles of inflammation, *Nature*. 454 (2008) 428–

435. <https://doi.org/10.1038/nature07201>.
- [2] W.W. Busse, L.J. Rosenwasser, Mechanisms of asthma, *J. Allergy Clin. Immunol.* 111 (2003) S799–S804. <https://doi.org/10.1067/mai.2003.158>.
- [3] G.K. Hansson, Inflammation, Atherosclerosis, and coronary artery disease, *N. Engl. J. Med.* 352 (2005) 1685–1695. <https://doi.org/10.1056/NEJMra043430>.
- [4] A. Mantovani, P. Allavena, A. Sica, F. Balkwill, Cancer-related inflammation, *Nature*. 454 (2008) 436–444. <https://doi.org/10.1038/nature07205>.
- [5] G.S. Hotamisligil, Inflammation and metabolic disorders, *Nature*. 444 (2006) 860–867. <https://doi.org/10.1038/nature05485>.
- [6] B. Samuelsson, S. Dahlen, J. Lindgren, C. Rouzer, C. Serhan, Leukotrienes and lipoxins: structures, biosynthesis, and biological effects, *Science* (80-.). 237 (1987) 1171–1176. <https://doi.org/10.1126/science.2820055>.
- [7] O. Rådmark, O. Werz, D. Steinhilber, B. Samuelsson, 5-Lipoxygenase, a key enzyme for leukotriene biosynthesis in health and disease, *Biochim. Biophys. Acta - Mol. Cell Biol. Lipids.* 1851 (2015) 331–339. <https://doi.org/10.1016/j.bbalip.2014.08.012>.
- [8] O. Werz, D. Steinhilber, Therapeutic options for 5-lipoxygenase inhibitors, *Pharmacol. Ther.* 112 (2006) 701–718. <https://doi.org/10.1016/j.pharmthera.2006.05.009>.
- [9] G.W. Carter, P.R. Young, D.H. Albert, J. Bouska, R. Dyer, R.L. Bell, J.B. Summers, D.W. Brooks, 5-lipoxygenase inhibitory activity of zileuton., *J. Pharmacol. Exp. Ther.* 256 (1991) 929–937. <http://jpet.aspetjournals.org/content/256/3/929.short>.
- [10] K.I. Kaitin, E.M. Healy, The new drug approvals of 1996, 1997, and 1998: Drug development trends in the user fee era, *Drug Inf. J.* 34 (2000) 1–14. <https://doi.org/10.1177/009286150003400101>.
- [11] C. Pergola, O. Werz, 5-Lipoxygenase inhibitors: a review of recent developments and patents, *Expert Opin. Ther. Pat.* 20 (2010) 355–375. <https://doi.org/10.1517/13543771003602012>.
- [12] B. Waltenberger, A.G. Atanasov, E.H. Heiss, D. Bernhard, J.M. Rollinger, J.M. Breuss, D. Schuster, R. Bauer, B. Kopp, C. Franz, V. Bochkov, M.D. Mihovilovic, V.M. Dirsch, H. Stuppner, Drugs from nature targeting inflammation (DNTI): A successful Austrian interdisciplinary network project, *Monatsh. Chem.* 147 (2016) 479–491.

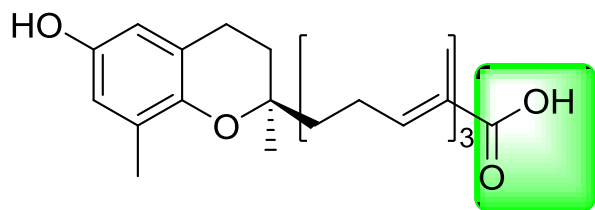
<https://doi.org/10.1007/s00706-015-1653-y>.

- [13] P. Richomme, J.-J. Helesbeux, D. Guilet, D. Seraphin, H. Stuppner, B. Waltenberger, D. Schuster, V.S. Temml, A. Koeberle, O. Werz, Tocotrienol derivatives, pharmaceutical composition and method of use in 5-lipoxygenase related diseases, WO 2017/032881 A1, 2017.
- [14] K. Alsabil, S. Suor-Cherer, A. Koeberle, G. Viault, A. Lavaud, V. Temml, B. Waltenberger, D. Schuster, M. Litaudon, S. Lorkowski, R. de Vaumas, J.-J. Helesbeux, D. Guilet, H. Stuppner, O. Werz, D. Seraphin, P. Richomme, Semisynthetic and natural garcinoic acid isoforms as new mPGES-1 inhibitors, *Planta Med.* 82 (2016) 1110–1116. <https://doi.org/10.1055/s-0042-108739>.
- [15] H.M. Evans, K.S. Bishop, On the existence of a hitherto unrecognized dietary factor essential for reproduction, *Science* (80-.). 56 (1922) 650–651. <https://doi.org/10.1126/science.56.1458.650>.
- [16] J.F. Pennock, F.W. Hemming, J.D. Kerr, A reassessment of tocopherol chemistry, *Biochem. Biophys. Res. Commun.* 17 (1964) 542–548. [https://doi.org/10.1016/0006-291X\(64\)90062-2](https://doi.org/10.1016/0006-291X(64)90062-2).
- [17] H. Pein, A. Ville, S. Pace, V. Temml, U. Garscha, M. Raasch, K. Alsabil, G. Viault, C. Dinh, D. Guilet, F. Troisi, K. Neukirch, S. König, R. Bilancia, B. Waltenberger, H. Stuppner, M. Wallert, S. Lorkowski, C. Weinigel, S. Rummler, M. Birringer, F. Roviezzo, L. Sautebin, J. Helesbeux, D. Séraphin, A.S. Mosig, D. Schuster, A. Rossi, P. Richomme, O. Werz, A. Koeberle, Endogenous metabolites of vitamin E limit inflammation by targeting 5-lipoxygenase, *Nat. Commun.* 9 (2018) 3834. <https://doi.org/10.1038/s41467-018-06158-5>.
- [18] D. Bartolini, F. De Franco, P. Torquato, R. Marinelli, B. Cerra, R. Ronchetti, A. Schon, F. Fallarino, A. De Luca, G. Bellezza, I. Ferri, A. Sidoni, W.G. Walton, S.J. Pellock, M.R. Redinbo, S. Mani, R. Pellicciari, A. Gioiello, F. Galli, Garcinoic acid is a natural and selective agonist of pregnane X receptor, *J. Med. Chem.* (2020) acs.jmedchem.0c00012. <https://doi.org/10.1021/acs.jmedchem.0c00012>.
- [19] F. Galli, A. Azzi, M. Birringer, J.M. Cook-Mills, M. Eggersdorfer, J. Frank, G. Cruciani, S. Lorkowski, N.K. Özer, Vitamin E: Emerging aspects and new directions, *Free Radic. Biol. Med.* 102 (2017) 16–36. <https://doi.org/10.1016/j.freeradbiomed.2016.09.017>.

- [20] M.L. Verdonk, J.C. Cole, M.J. Hartshorn, C.W. Murray, R.D. Taylor, Improved protein–ligand docking using GOLD, *Proteins Struct. Funct. Bioinforma.* 52 (2003) 609–623. <http://onlinelibrary.wiley.com/doi/10.1002/prot.10465/full>.
- [21] O. Korb, T. Stutzle, T.E. Exner, Empirical scoring functions for advanced protein–ligand docking with PLANTS, *J. Chem. Inf. Model.* 49 (2009) 84–96. <http://pubs.acs.org/doi/abs/10.1021/ci800298z>.
- [22] L. Schmölz, M. Birringer, S. Lorkowski, M. Wallert, Complexity of vitamin E metabolism, *World J. Biol. Chem.* 7 (2016) 14–43. <https://doi.org/10.4331/wjbc.v7.i1.14>.
- [23] A. Ville, G. Viault, J.J. Hélesbeux, D. Guilet, P. Richomme, D. Séraphin, Efficient semi-synthesis of natural δ -(R)-tocotrienols from a renewable vegetal source, *J. Nat. Prod.* 82 (2019) 51–58. <https://doi.org/10.1021/acs.jnatprod.8b00517>.
- [24] J.C. Sheehan, G.P. Hess, A new method of forming peptide bonds, *J. Am. Chem. Soc.* 77 (1955) 1067–1068. <https://doi.org/10.1021/ja01609a099>.
- [25] E. Valeur, M. Bradley, Amide bond formation: beyond the myth of coupling reagents, *Chem. Soc. Rev.* 38 (2009) 606–631. <https://doi.org/10.1039/B701677H>.
- [26] R. Knorr, A. Trzeciak, W. Bannwarth, D. Gillessen, New coupling reagents in peptide chemistry, *Tetrahedron Lett.* 30 (1989) 1927–1930. [https://doi.org/10.1016/S0040-4039\(00\)99616-3](https://doi.org/10.1016/S0040-4039(00)99616-3).
- [27] C.N. Serhan, Resolution phase of inflammation: novel endogenous anti-inflammatory and proresolving lipid mediators and pathways, *Annu. Rev. Immunol.* 25 (2007) 101–137. <https://doi.org/10.1146/annurev.immunol.25.022106.141647>.
- [28] C.N. Serhan, Pro-resolving lipid mediators are leads for resolution physiology, *Nature.* 510 (2014) 92–101. <https://doi.org/10.1038/nature13479>.
- [29] N.C. Gilbert, S.G. Bartlett, M.T. Waight, D.B. Neau, W.E. Boeglin, A.R. Brash, M.E. Newcomer, The structure of human 5-lipoxygenase, *Science* (80-.). 331 (2011) 217–219. <https://doi.org/10.1126/science.1197203>.
- [30] H.M. Berman, T. Battistuz, T.N. Bhat, W.F. Bluhm, P.E. Bourne, K. Burkhardt, Z. Feng, G.L. Gilliland, L. Iype, S. Jain, P. Fagan, J. Marvin, D. Padilla, V. Ravichandran, B. Schneider, N. Thanki, H. Weissig, J.D. Westbrook, C. Zardecki, The protein data

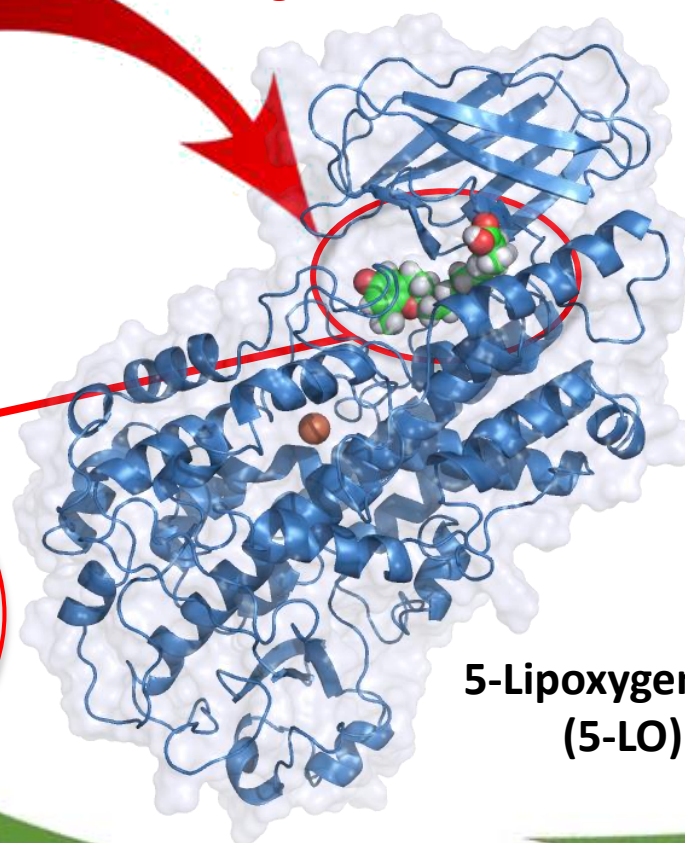
- bank, *Acta Crystallogr. Sect. D Biol. Crystallogr.* 58 (2002) 899–907. <https://doi.org/10.1107/S0907444902003451>.
- [31] O. Guner, O. Clement, Y. Kurogi, Pharmacophore Modeling and three dimensional database searching for drug design using catalyst: recent advances, *Curr. Med. Chem.* 11 (2012) 2991–3005. <https://doi.org/10.2174/0929867043364036>.
- [32] G. Wolber, T. Langer, LigandScout: 3-D Pharmacophores derived from protein-bound ligands and their use as virtual screening filters, *J. Chem. Inf. Model.* 45 (2005) 160–169. <https://doi.org/10.1021/ci049885e>.

Potent natural 5-LO inhibitor

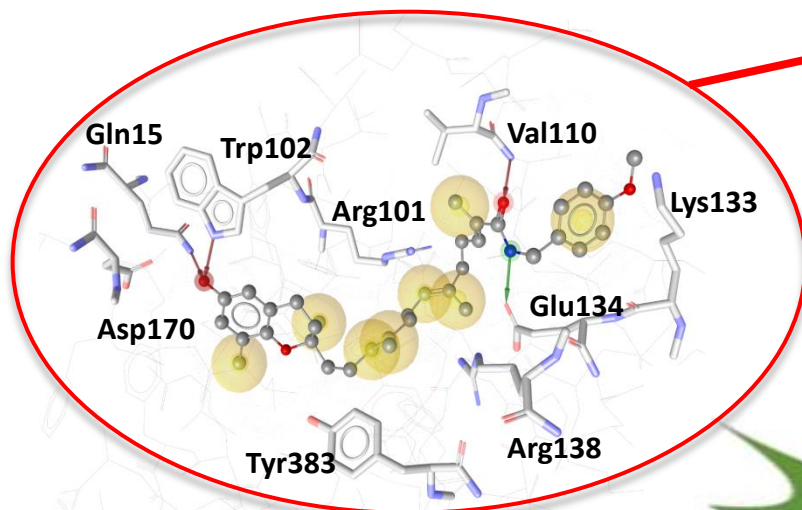


δ -Garcinoic acid (δ -GA)

Docking

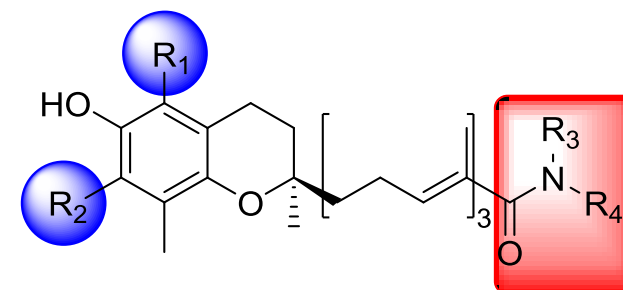


5-Lipoxygenase (5-LO)



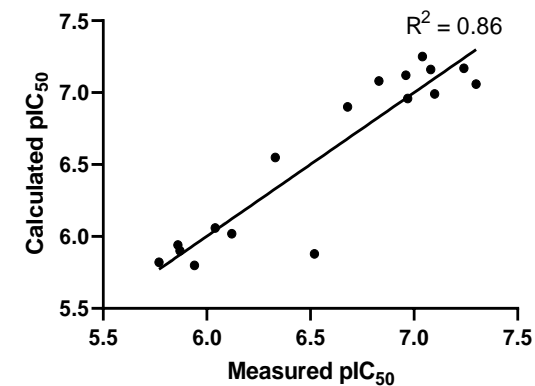
Allosteric binding site

Scoring



24 garcinamides

in silico design and semi-synthesis of amide analogues of GA isoforms



Semi-quantitative prediction model